OPEN ACCESS

Clay mineral-grain size-calcite cement relationships in the Upper Cretaceous Chalk, UK: a preliminary investigation

C. V. JEANS[1],*, N. J. TOSCA[2], X. F. HU[3] AND S. BOREHAM[1]

[1] *Department of Geography, University of Cambridge, Downing Place, Cambridge, CB2 3EQ, UK,* [2] *Department of Earth Sciences, University of St Andrews, St Andrews, KY16 9AL, UK,* [3] *Editorial Office of Journal of Palaeogeography, China University of Petroleum (Beijing), 20 Xueyuan Road, P.O. Box 902, Beijing 100083, China*

ABSTRACT: The idea is tested that the evolution of the Chalk's clay mineral assemblage during diagenesis can be deduced by examining the relationships between its clay mineralogy, particle size distribution pattern, and the timing and trace element chemistry of the calcite cement. The preliminary results from five different examples of cementation developed at different stages of diagenesis in chalks with smectite-dominated clay assemblages suggest that this is a promising line of investigation. Soft chalks with minor amount of anoxic series calcite cement poor in Mg, Fe and Mn are associated with neoformed trioctahedral smectite and/or dioctahedral nontronite and talc. Hard ground chalk with extensive anoxic series calcite cement enriched in Mg and relatively high Fe, Mn and Sr are associated with neoformed glauconite *sensu lato*, berthierine and dioctahedral smectite, possibly enriched in Fe. The chalk associated with large ammonites shows extensive suboxic series calcite cement enriched in Mg, Mn and Fe that show no obvious correlation with its clay mineralogy. Nodular chalks with patchy suboxic series calcite cement enriched in Fe are associated with neoformed dioctahedral smectite, possibly enriched in Al, and berthierine. Regionally hardened chalk with extensive suboxic calcite cement and relatively high trace element contents contain pressure dissolution seams enriched in kaolin and berthierine. Laser-based particle-size distribution patterns suggest that each type of lithification has a typical complex clay mineral population, indicating that subtleties in mineralogy are not being identified and that there could be some control on the size and shape of the clay crystals by the different types of cementation.

KEYWORDS: chalk, Upper Cretaceous, clay minerals, grain size, calcite cement, trace elements, neoformation, diagenesis.

The abundant and characteristic smectitic phase (smectite and smectite-rich illite-smectite) that dominates the clay assemblages of the Upper Cretaceous Chalk is not a homogenous mineral (Deconinck & Chamley, 1995; Drits *et al.*, 1998, 2004; Lindgreen *et al.*, 2002, 2008). A summary (Jeans, 2006) emphasizes the considerable variation in its XRD profile, the degree of expandability with glycerol and the extent of its collapse at 400ºC and 550ºC heating and concludes that the Chalk smectite is a heterogenous mixture of different collapsible phases. Hu *et al.* (2014) have suggested these differences as well as other variations in the Chalk's clay assemblage may be related in part to the diagenetic history of the Chalk and in particular to the various phases of lithification and the chemistry of the calcite cement. Our study is

based upon the idea that the Chalk can be treated as a giant calcite-cemented nodule (Hu *et al.*, 2014) as long as it is realized that there are also variations in the Chalk's clay mineral assemblage that are related to regional variations in the detrital sources and the physical conditions of deposition and not to diagenesis. In this investigation we explore this concept in five examples of Chalk from southern and eastern England that have been lithified by calcite cementation at various stages during their diagenesis. These range from soft chalks of Campanian age with little obvious cement and a minor clay mineral content (1−2%), representing a very distal facies in the Chalk Sea, to examples of chalks of Cenomanian age with higher clay mineral contents (up to ~ 15%) representing more extensive cementation in a more proximal and perhaps shallower water environment; the latter are associated with hardgrounds, preferential lithification relating to large ammonites originally buried in the chalk sediment, nodular development and regional hardening. Relationships have been explored between the variation in clay mineralogy of different size clay fractions, the timing and geochemistry of the cement, and how these may both be reflected in the particle size distribution pattern determined by laser diffraction − a technique that provides a different, but potentially very revealing view of the variation in particle shape, size and association that may reflect the complexities of the smectite-rich Chalk assemblage, not easily seen by other methods. The effect of calcite cementation is two-fold. It may stop or restrict reactions taking place between the evolving clay mineral assemblage and the porewaters of the sediment. It may preferentially remove from solution cations such as Mg and Fe that are important for various clay-mineral-forming reactions as they are preferentially incorporated in the calcite structure.

Preliminary analysis of the <2 μm clay fractions from these five specific examples of lithified chalk suggest that a smectitic phase and mica are the dominant components. Kaolinite may be present in the Cenomanian chalks from eastern England but it is absent from the younger Campanian Chalk in southern England.

Figure 1 shows the locations mentioned in the text, Fig. 2 shows the stratigraphical scheme used, as well as the sample levels (more precise stratigraphical details of the samples from Speeton are provided in Jeans, 1980, fig. 16).

ANALYTICAL METHODS

Acid-insoluble residues were extracted from chalk by dissolving roughly crushed samples in cold 1 molar acetic acid. After washing with deionized water, the acid insoluble residues were dispersed in 0.1% sodium hexametaphosphate solution buffered at pH 3. The suspension was split into two or three portions. The first was used to measure the general particle size distribution. The second was split into <0.2 μm e.s.d., 0.2−1 μm e.s.d. and 1−2 μm e.s.d. size fractions using centrifugally enhanced settling over 45 cm for the finest two fractions, and gravitational settling for the 1−2 μm e.s.d. fraction over 65 to 83 cm depending on the concentration of the suspension. The third was kept as a reserve. The three particle size fractions separated by settling are differentiated from those measured by the laser particle size analyser (Mastersizer, 2000) by the postscript e.s.d. (effective settling diameter) to avoid confusion. Particle size distribution analysis was carried out on the three separated clay fractions and the total acid insoluble residue with Malvern's Mastersizer 2000 under standardized conditions. The dispersant was deionized water, pump speed was 2250 rpm, ultrasonic agitator at 4.8 μm displacement, and obscuration ranged from 2 to 20%. Three runs, each of 3 minutes, were carried out on every sample to check the stability of the suspension. The first was without ultrasonic action, the second and third runs were with ultrasonic agitation. Evidence of considerable instability was evident in some samples during the initial run, whereas stability was established with the ultrasonic treatment. The particle size distribution patterns used in our study are the averages of the three measurements made on the third run. The Malvern Mastersizer 2000 uses a totally different method of estimating particle size. It is not based on gravitation settling but on measuring the intensity of light scattered as a laser beam passes through the dispersed particulate sample. Typically for fully dispersed suspensions of particles of the same shape and density, the laser diffraction method will record larger diameter particles than gravitation settling methods. The extent of the difference is related to the shape of the particles. With increasing aspect ratios of the particles the larger will be the difference.

Trace element content (Fe, Mn, Mg, Sr) of the bulk calcite from the total sample and the separated <2 μm fraction of chalk from Peacehaven were
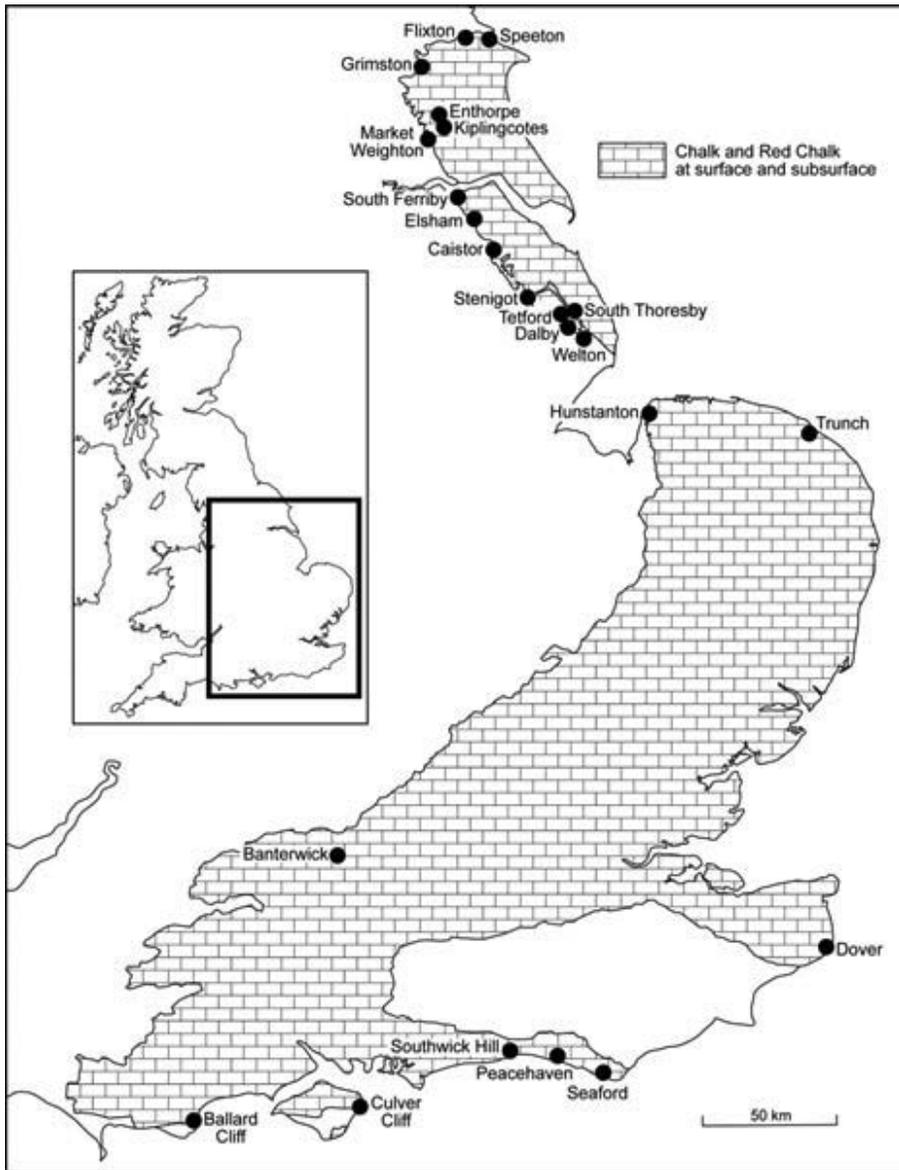
Fig. 1. Distribution of the Upper Cretaceous Chalk in the UK showing locations mentioned in the text.

determined using a Perkin-Elmer ICP-OES in the Department of Geography, University of Cambridge. Additional details of the sample preparation procedure are given in Jeans *et al.* (2012, p. 188) and Hu *et al.* (2014). The chemistry of its cement was modelled graphically by comparing the cross plots of the trace element (Fe, Mn, Mg, Sr) and the C^{12}/C^{13} of the bulk calcite of the total sample with that of the separated <2 μm calcite fraction and the predicted C^{12}/C^{13} values for the cement using the data in Jeans *et al.* (2012, tables 7−9, fig. 16).

The **Standard Louth Chalk** of Jeans *et al.* (2012) has been used in modelling the volume of cement in the five different examples of lithification. It is considered to be a fully compacted
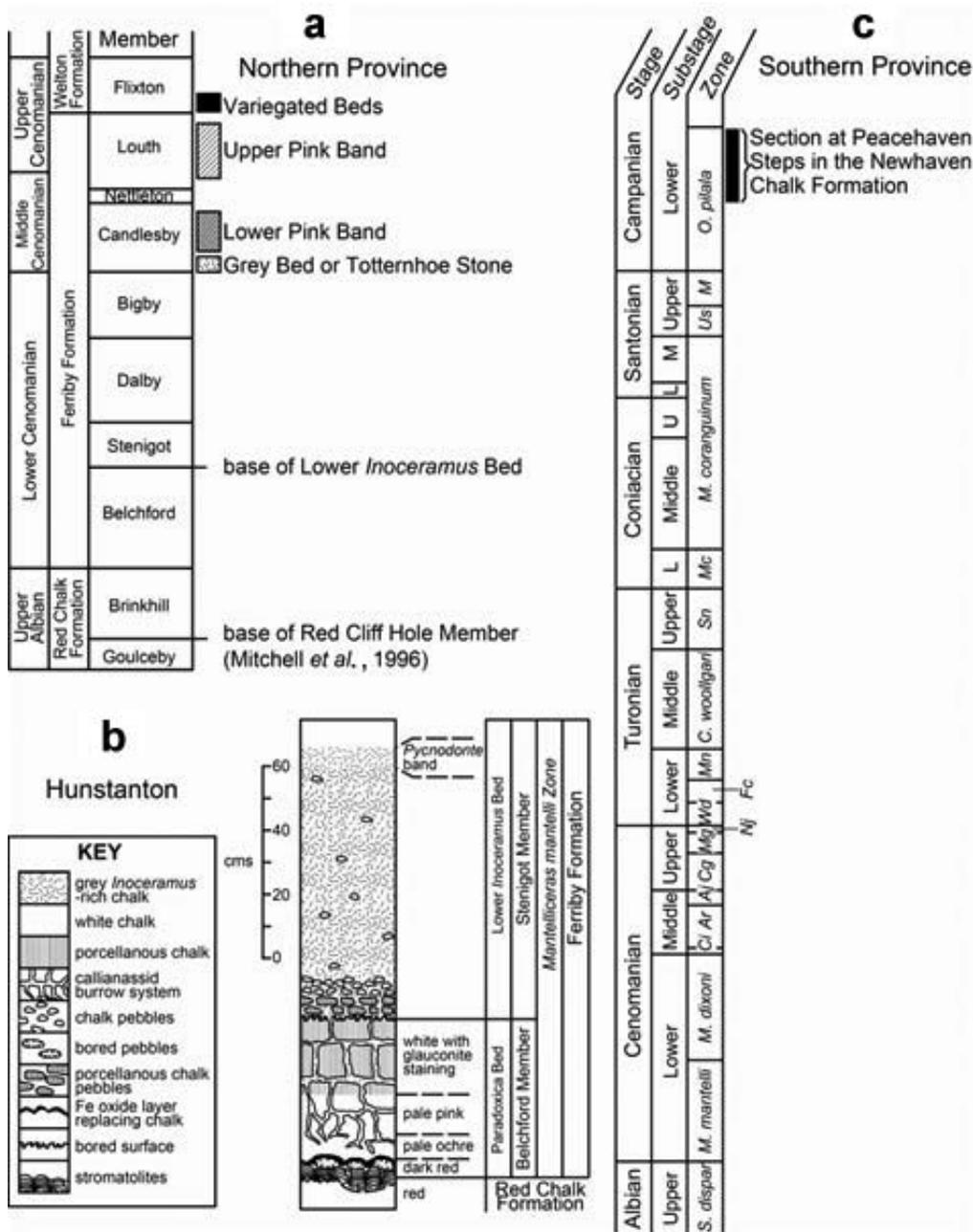
FIG. 2. Stratigraphical schemes used for the description and location of samples.

uncemented chalk unaffected by early lithification and any appreciable pressure dissolution. It is based upon the average of a number of samples from the Upper Cenomanian Louth Chalk Member at Dover. The bulk specific gravity is 1.65, the acid insoluble residue is 4 vol.%, the CaCO$_3$ content is 56 volume percent and the porosity is 40 vol.%. The trace element content (Fe 255 ppm; Mn 330 ppm; Mg 1312 ppm; Sr 550 ppm) of the calcite in the Standard Louth Chalk was used to model the

cement chemistry of the regionally hardened chalk of the Louth Member (Ferriby Formation) at Speeton, using its present trace element chemistry.

For XRD mineralogical analyses subsamples of the <0.2 μm, 0.2−1 μm and 1−2 μm clay suspensions were flocculated with concentrated $CaCl_2$ solution, filtered, and transferred to glass slips to form oriented aggregates on drying. Another part of the clay filtrate was dried, finely chopped up with a razor, mounted on double-sided sellotape and stuck to a glass slip to form unoriented clay preparations. X-ray diffraction analysis was carried out using a Siemens D5000 over the range 2 to 32º2θ for oriented samples and 58 to 64º2θ for random samples at 0.25º2θ per minute.

Identification of the clay mineral assemblages was conducted using air dried, glycolated, and 400ºC and 550ºC heat-treated (2 h) oriented aggregate specimens. In addition, for <0.2 μm size fractions, randomly oriented aggregates were analysed from 58−64º2θ to resolve weak 060 reflections. These latter reflections were used in an attempt to distinguish between trioctahedral and dioctahedral varieties. Smectite or smectite-rich I/S was identified by expansion of the 001 peak upon glycol treatment to ~17 Å. We use the term smectite for a phase with diffraction characteristics of 85% or higher smectite in a illite/smectite phase. Figure 3a compares the 060 reflections of the two associations of smectite that we have identified. Sample PHS11 has a main 060 peak at 1.49 Å and a shoulder at 1.52 Å; this is interpreted as a mixture of a dominant dioctahedral smectite with a lesser amount of a trioctahedral smectite and/or dioctahedral nontronite. Sample R8 has an 060 peak at 1.49 Å, indicating the presence of only dioctahedral smectite. Details of the 060 reflections were only recorded from the <0.2 μm fractions; for the 0.2−1 μm and 1−2 μm fractions the generic term smectite is used in our descriptions. Mica (illite) was identified by the presence of the 001 peak at ~10 Å and a lack of expansion upon glycol treatment. Kaolinite and berthierine were identified by the 001 peak at ~7.1 Å, with collapse of this peak at 400ºC indicating berthierine, and collapse of the peak at 550ºC indicating kaolinite (Fig. 3b). Chlorite was identified by the presence of the 001 peak at ~14.2 Å and the 002 peak at ~7 Å, with positive identification made possible by intensity increases of the 001 peak after heating to 550ºC.

In the 0.2−1 μm and 1−2 μm fractions from the Peacehaven samples there is a peak at ~9.2 Å which shows no response to glycol treatment or heating. In addition, peaks are present at 4.59, 4.24 and 3.06 Å (Fig. 3c). The combination of 9.2, 4.59 and 3.06 Å peaks is consistent with the presence of talc. However the presence of the additional peak at 4.24 Å may indicate pyrophyllite instead. Indirect evidence supports the presence of talc with the 4.24 Å peak related to small amounts of feldspar. Figure 3c shows that the intensity of the 4.24 Å peak is independent of the 9.2 Å peak; the most intense 4.24 Å peak is associated with sample PHS26, a sample with an exceptionally high feldspar content in the >2 μm fraction (Fig. 4).

Mineral percentages were estimated for <0.2 μm, 0.2−1 μm, and 1−2 μm fractions using a forward modelling approach by simulating the one dimensional powder X-ray diffraction patterns using the software program *NEWMOD* (Reynolds & Reynolds, 1996). The calculation of X-ray diffraction patterns used parameters from diffraction experiments, namely: a Cu-$K\alpha_1$ radiation source, a 20 cm goniometer radius, Soller slit effective axial divergence values of 6.6 and 2º, a 1.9 cm sample length, and a 3×10^4 counts per second quartz reference intensity. Absolute *d* spacing values were calibrated periodically on the Siemens D5000 using prepared thin films of crystallized *n*-tetradecanol, which produces regularly spaced, consistent diffraction peaks to very large *d* spacing (Brindley & Wan, 1974). Upon calculating nearly pure smectite phases in the <0.2 μm fraction, we applied a defect broadening particle size distribution to match peak breadth and position as accurately as possible. Then, this phase was included in subsequent grain size fractions in addition to new phases such as kaolinite, talc, etc. All samples were compared to calculated patterns in the expanded state with ethylene glycol. Matches between calculated and observed patterns also focused on low-intensity basal spacings at smaller *d* spacing to estimate roughly the Fe-content and relative abundance. In this way, mineral abundances of our samples are considered to be internally consistent.

RESULTS

Soft chalk at Peacehaven, Sussex

The samples came from a 15 m section of soft chalk of Campanian age (*Offaster pilula* zone) exposed in the sea cliffs at Peacehaven, Sussex (Hu *et al.*, 2014, fig. 13). Details of the lithological
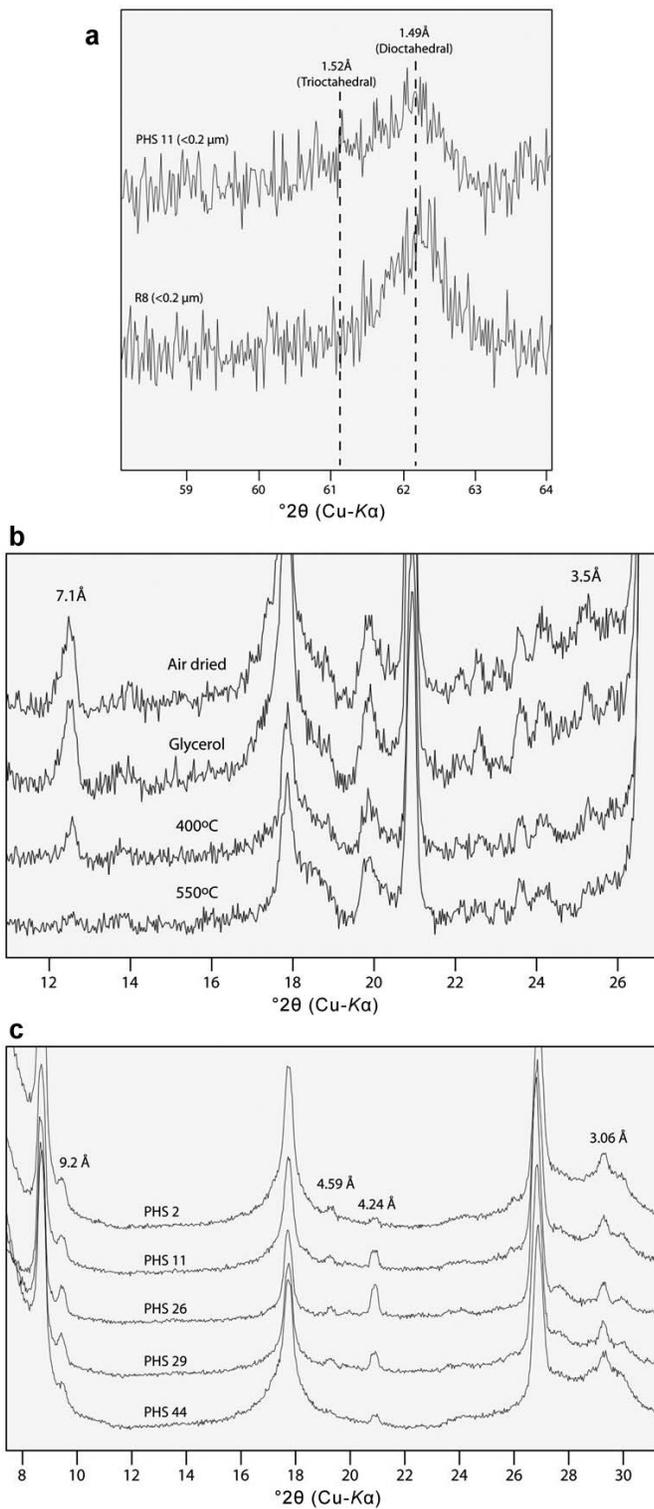
section, sample levels, values of O^{16}/O^{18} (calcite) and C^{12}/C^{13} (calcite), and bulk density are provided in Jeans *et al.* (2012). The following six samples out of the original 65 that underwent preliminary mineralogical analysis of their clay fractions were selected for detailed investigation:

> PHS 2. Old Nore Marl. 89.5% $CaCO_3$. A marl 10 cm thick of very wide extent with a marked *negative* europium anomaly in its acid-insoluble residue; considered to be of volcanic origin.
>
> PHS 44. Meeching Marl. 93.2% $CaCO_3$. A marl 35 cm thick of wide extent lacking a negative europium anomaly, considered to be of detrital origin.
>
> PHS 26. chalk. 99% $CaCO_3$ (Fig. 4). The acid insoluble residue contains numerous minute alkali feldspar crystals, considered to represent a fine-grained crystal ash fall.
>
> PHS 11. chalk. 98.8% $CaCO_3$.
>
> PHS 29. chalk. 98.8% $CaCO_3$.
>
> PHS 32. chalk. 98.8% $CaCO_3$.

Volume and chemistry of calcite cement. The bulk density of the Peacehaven Chalk ranges from 1.63 to 1.85 not including the marls (Jeans *et al.*, 2012). The lower value is similar to the **Standard Louth Chalk** with a 40% porosity, whereas the upper value 1.85 indicates 6 vol.% of calcite cement. The chemistry of this cement was modelled using the data shown in Table 1. The modelled calcite cement ranges in Fe from 55 to 180 ppm, Mn from 5 to 100 ppm, Mg from ~0 to 300 ppm, and Sr from ~150 to 620 ppm. Jeans *et al.* (2012) have demonstrated that this cement belongs to the anoxic cement series of Hu *et al.* (2012). Compared to the calcite cements in the Cenomanian Chalks of eastern England the concentrations of Fe, Mn and Mg are lower by at least an order of magnitude (Hu *et al.*, 2012).

Clay mineralogy. The clay mineral analyses of the <0.2 μm, 0.2−1 μm and 1−2 μm fractions are given in Table 2. The <0.2 μm fractions of all six samples are dominated by smectite(>90%), predominantly dioctahedral, with either nontronite or some trioctahedral phase (Fig. 3a), with very minor
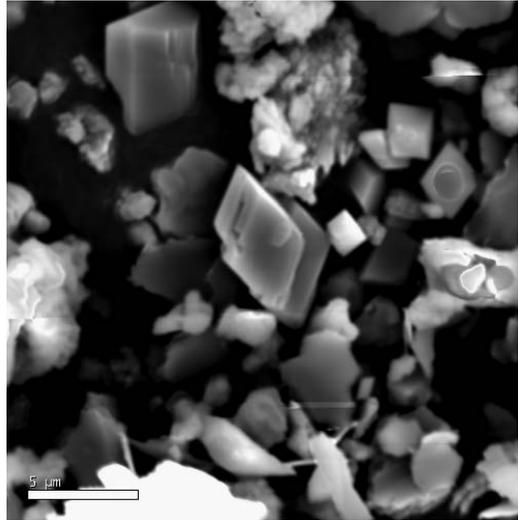

Fig. 4. Abundant euhedral crystals of alkali feldspar (very low in Na with a K:Ca ratio of 10) in the >2 μm e.s.d. acid insoluble fraction of sample PHS26, Campanian Chalk, *Offaster pilula* zone, Peacehaven, Sussex.

or trace amounts of mica. The collapse of the 001 smectite peak on 400ºC heating is incomplete, varying from sample to sample (Fig. 5). The 0.2−1 μm fraction is dominated by smectite (58−85%) but mica (up to 23%) and talc (up to 19%) are appreciable components. The collapse of the 001 smectite peak from the 0.2−1 μm fraction on 400ºC heating is variable and does not necessarily coincide with the pattern exhibited by the <0.2 μm fraction. The 1−2 μm fraction is only represented by the two marl bands, PHS 2, PHS 44. The clay mineralogy is dominated by mica (50−56%) with lesser amounts of smectite (29−38%) and talc (12−15%).

Particle size distribution patterns. The <0.2 μm e.s.d. fractions (Fig. 6) display two grain populations, the dominant one centred on 0.2 μm and sometimes a minor but broad one extending from 1.05 to 13 μm. The pattern of variation shows no

Fig. 3 (*facing page*). XRD patterns of clay assemblages showing; (a) the 060 diffraction peaks characteristic of the <0.2 μm e.s.d. fractions of trioctahedral smectite (or nontronite) at ~1.52 Å and dioctahedral smectite at 1.49 Å from Peacehaven (PHS11) and the dioctahedral smectite from Hunstanton and Speeton (R8); (b) the 0.2−1 μm e.s.d fraction of the nodule F6 from Speeton showing the decrease in the intensity of the 7 Å peak on 400ºC heating, indicating the presence both kaolinite and berthierine; and (c) the 0.2−1 μm e.s.d. fractions from the samples from Peacehaven showing the presence of talc.

C. V. Jeans et al.

TABLE 1. Estimated $\delta^{13}C$ values of the calcite cement, and trace element concentrations and $\delta^{13}C$ values of the bulk calcite in the total and <2 μm fractions of chalk samples from the *Offaster pilula* zone of the Newhaven Chalk Formation at Peacehaven, Sussex, UK.

| Sample	$\delta^{13}C$ (‰) <2 μm	$\delta^{13}C$ (‰) Total	Estimated cement $\delta^{13}C$ (‰)	Fe (ppm) <2 μm	Fe (ppm) Total	Mn (ppm) <2 μm	Mn (ppm) Total	Mg (ppm) <2 μm	Mg (ppm) Total	Sr (ppm) <2 μm	Sr (ppm) Total
PHS 8	−4.9	1.92	−10	90	91	140	321	1219	2836	584	530
PHS 16	−3.8	2.3	−7.5	118	69	155	222	1254	2172	464	764
PHS 32	−8.3	2.27	−11	58	71	96	200	930	4585	391	788
PHS 33	−1.65	2.15	−7.5	82	67	163	219	1484	3186	531	732
PHS 45	−7.2	2.13	−11	70	85	134	223	1121	3821	364	848
PHS 51	−2.05	2.07	−11	75	108	136	264	1227	3948	434	669
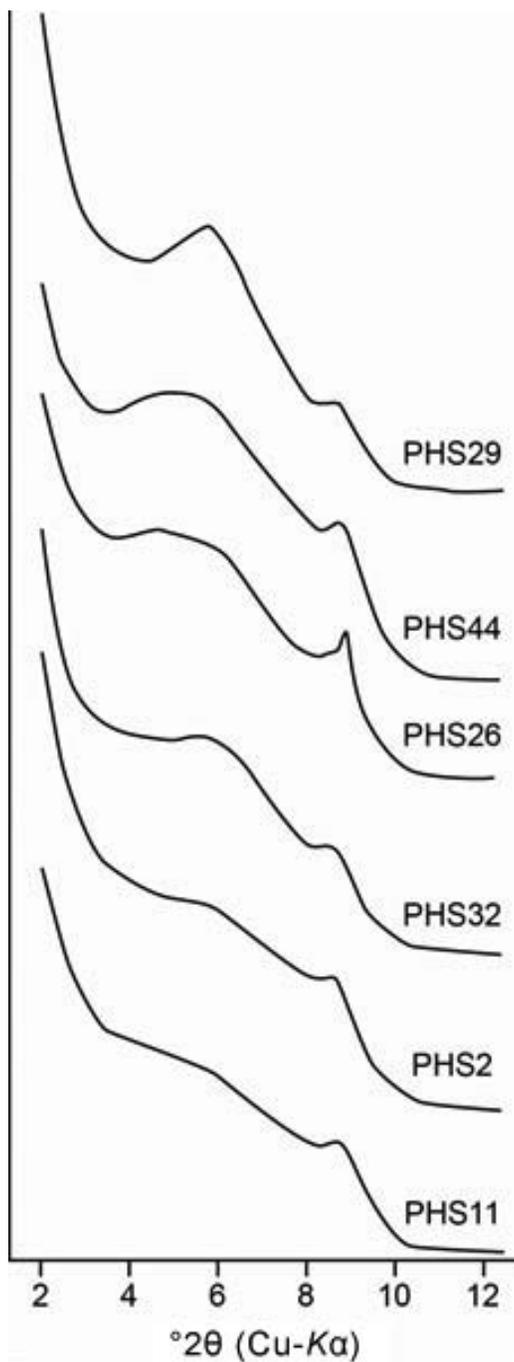
FIG. 5. XRD patterns of the 400°C heated <0.2 μm e.s.d. fractions of the Peacehaven samples arranged to show the different degrees of collapse of the smectitic peak.

TABLE 2. Clay mineralogy of chalk samples from the *Offaster pilula* zone of the Newhaven Chalk Formation at Peacehaven, Sussex, UK.

Sample	Size fraction (μm)	Smectite (%)	Mica (%)	Talc (%)
PHS2	<0.2	100	tr	–
PHS11	<0.2	100	tr	–
PHS26	<0.2	95	5	–
PHS29	<0.2	100	tr	–
PHS32	<0.2	97	3	–
PHS44	<0.2	100	tr	–
PHS2	0.2 to 1	76	12	12
PHS11	0.2 to 1	76	12	12
PHS26	0.2 to 1	58	23	19
PHS29	0.2 to 1	70	15	15
PHS32	0.2 to 1	64	19	17
PHS44	0.2 to 1	85	8	7
PHS2	1 to 2	29	56	15
PHS44	1 to 2	38	50	12

obvious correlation with mineral composition. The 0.2−1 μm e.s.d. fractions display the same two populations (Fig. 6) but the one centred at 0.2 μm is much reduced, whereas the broad one (0.4−13 μm) is often the larger and is usually dominated by particles in the 1.1−1.9 μm range. PHS 2 is exceptional as the broad population is dominated by 1.1−1.2 μm and 11 μm particles. The 1−2 μm e.s.d. fraction is represented only in the marl bands PHS 2 and PHS 44 (Fig. 7). Each has a small grain population centred at 0.25 μm representing residual material from the <0.2 μm fraction; the main population extending from 1.05 μm to 11 μm is dominated by particles of ~6 μm.

The Paradoxica Bed hardground at Hunstanton, Norfolk

The glauconite-stained Paradoxica Bed hardground is of Lower Cenomanian age (*Mantelliceras mantelli* zone) and occurs in the lower part of the Ferriby Chalk Formation in eastern England. At Hunstanton it exhibits very clearly the interrelationships between early lithification by calcite cementation, the presence of an undistorted callianassid burrow system lined with green clay that must have been open to the circulation of the Chalk's ambient seawater, and an association with the coeval dissolution of fine-grained $Fe(OH)_3$. Figure 8 is a schematic section through the Paradoxica Bed at Hunstanton, Norfolk, showing the position of samples studied, and its relationship to the underlying chalk. Further details are in Jeans (1980, pp. 101−106, 147−150), Gallois (1994, p. 124) and Hu *et al.* (2014, figs. 6, 11, 12).

Volume and chemistry of calcite cement. The bulk density of the chalk making up the body of Paradoxica Bed (not the burrow infills) ranges from 2.22 (18% porosity) in the lower part to 2.62 (3% porosity) in the uppermost part (Jeans, 1980, p. 103). Comparison to the **Standard Louth Chalk** indicates cement volumes from 37% to 22%. As lithification set in prior to the completion of primary compaction (burrows are still undistorted in the upper half of the bed) these estimated cement volumes must be minimum values.

Details of (a) the cement chemistry recorded in vugs inside brachiopods is given in Hu *et al.* (2012, terebratulids T12, T16), and (b) variations in the bulk chemistry of this hardground at Hunstanton and Stenigot in Hu *et al.* (2014, table 5) and Jeans *et al.* (2012, table 2). Of particular interest is the enhanced Mg content of the bulk calcite in the upper part of the Paradoxica Bed reflecting the Mg-enriched calcite (up to 4000 ppm) that is the earliest cement recognized; the Fe, Mn and Sr contents of the cements reach respectively values of 2700 ppm, 4800 ppm and 750 ppm.

Clay mineralogy. The clay mineral analyses of the <0.2 μm, 0.2−1 μm and 1−2 μm fractions are
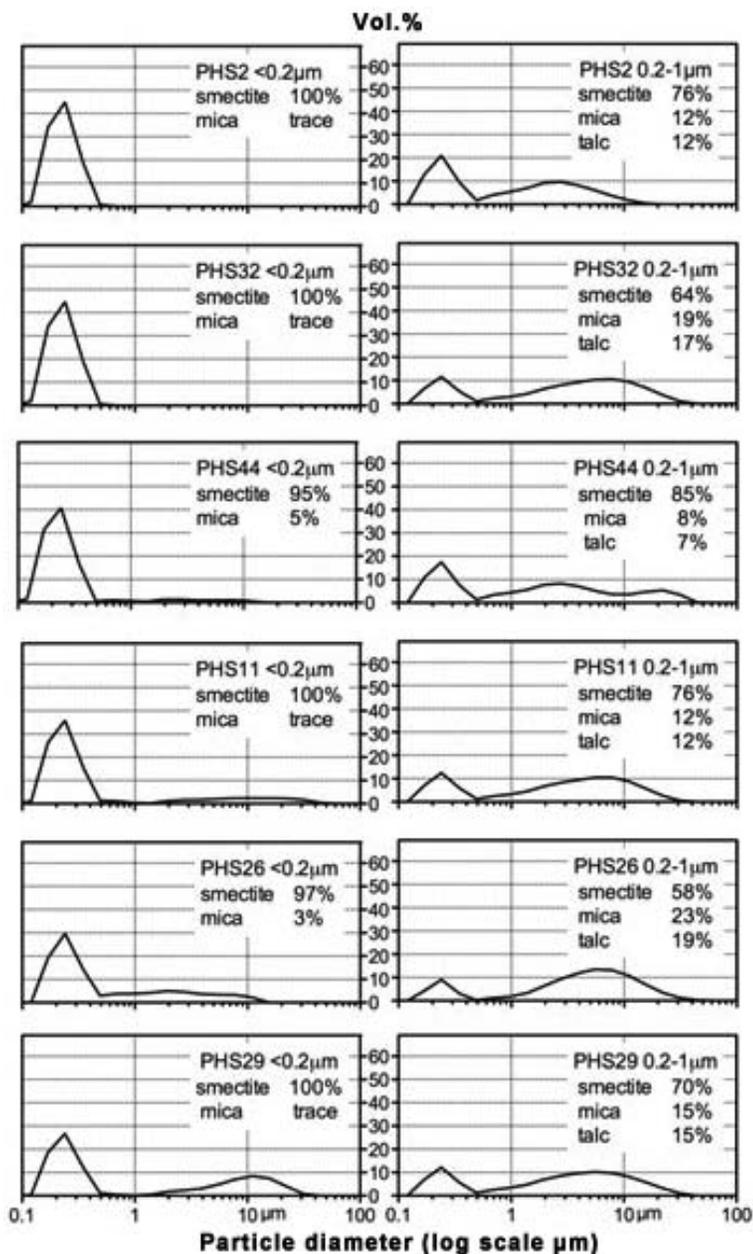
FIG. 6. Mastersizer particle size distribution patterns of the <0.2 μm e.s.d. and 0.2−1 μm e.s.d. fractions from the Peacehaven samples.

given in Table 3. The <0.2 μm clay mineralogy of the main body of the bed (NOR21-23, NOR27, 28) is dominated by dioctahedral smectite (49−62%) with kaolinite (27−36%) and mica (11−14%). The <0.2 μm fraction from the grey clay lining to the burrows (NOR24A) has a similar mineralogy,

whereas the green-clay lining (NOR23A) in the upper part of the Paradoxica Bed has a higher content of dioctahedral smectite (67%) and mica (17%) and lower kaolinite (16%). The 0.2−1 μm fraction of the main body of the bed is dominated by kaolinite (50−62%) with smectite (24−27%)
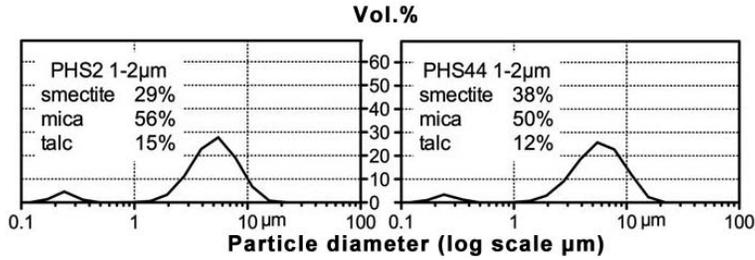
Fig. 7. Mastersizer particle size distribution patterns of the 1−2 μm e.s.d. fractions from the Old Nore Marl (PHS2) and the Meeching Marl (PHS44).

and mica (11−14%) with traces of berthierine and chlorite in some samples. The grey clay lining to the burrows display enhanced smectite (39−41%) and reduced kaolinite (35−50%). The green clay burrow lining (NOR23A) has an enhanced mica content (24%) relative to the samples from the main body of the bed and the grey clay burrow lining. Only five of the seven samples provided 1−2 μm fractions. The three lowest samples (NOR21-23) are dominated by kaolinite (38−40%) and chlorite (38−41%) with mica (19–20%) and traces of smectite. The highest sample of the Paradoxica

Bed, NOR28, and the grey clayey burrow lining have similar clay assemblages which are dominated by smectite (42−44%), mica (18−19%) and chlorite (trace−3%). The dioctahedral smectite of the <0.2 μm fraction displays the least general resistance to collapse on 400ºC heating (Fig. 9) compared to samples from Peacehaven and Speeton.

Particle size distribution patterns. Representative samples are illustrated in Figs 10 and 11. All the <0.2 μm e.s.d. fractions, except for NOR23A of the green clay burrow lining, are represented by a

TABLE 3. Clay mineralogy of chalk samples from the Paradoxica Bed hardground (*Mantelliceras mantelli* zone) of the Ferriby Formation at Hunstanton, Norfolk, UK.

| Sample	Size fraction (μm)	Smectite (%)	Mica (%)	Kaolinite (%)	Berthierine (%)	Chlorite (%)
NOR21	<0.2	49	15	36	−	−
NOR22	<0.2	56	13	31	−	−
NOR23	<0.2	62	10	28	−	−
NOR23A	<0.2	67	17	16	−	−
NOR24A	<0.2	60	11	29	−	−
NOR27	<0.2	62	11	27	−	−
NOR28	<0.2	62	11	27	−	−
NOR21	0.2 to 1	24	14	62	tr	tr
NOR22	0.2 to 1	27	13	60	−	tr
NOR23	0.2 to 1	24	14	62	−	tr
NOR23A	0.2 to 1	41	24	35	−	−
NOR24A	0.2 to 1	39	11	50	tr	tr
NOR27	0.2 to 1	24	14	62	−	tr
NOR28	0.2 to 1	39	11	50	−	−
NOR21	1 to 2	tr	20	40	−	40
NOR22	1 to 2	tr	19	40	−	41
NOR23	1 to 2	tr	20	38	4	38
NOR24A	1 to 2	44	18	35	−	3
NOR28	1 to 2	42	19	39	−	tr
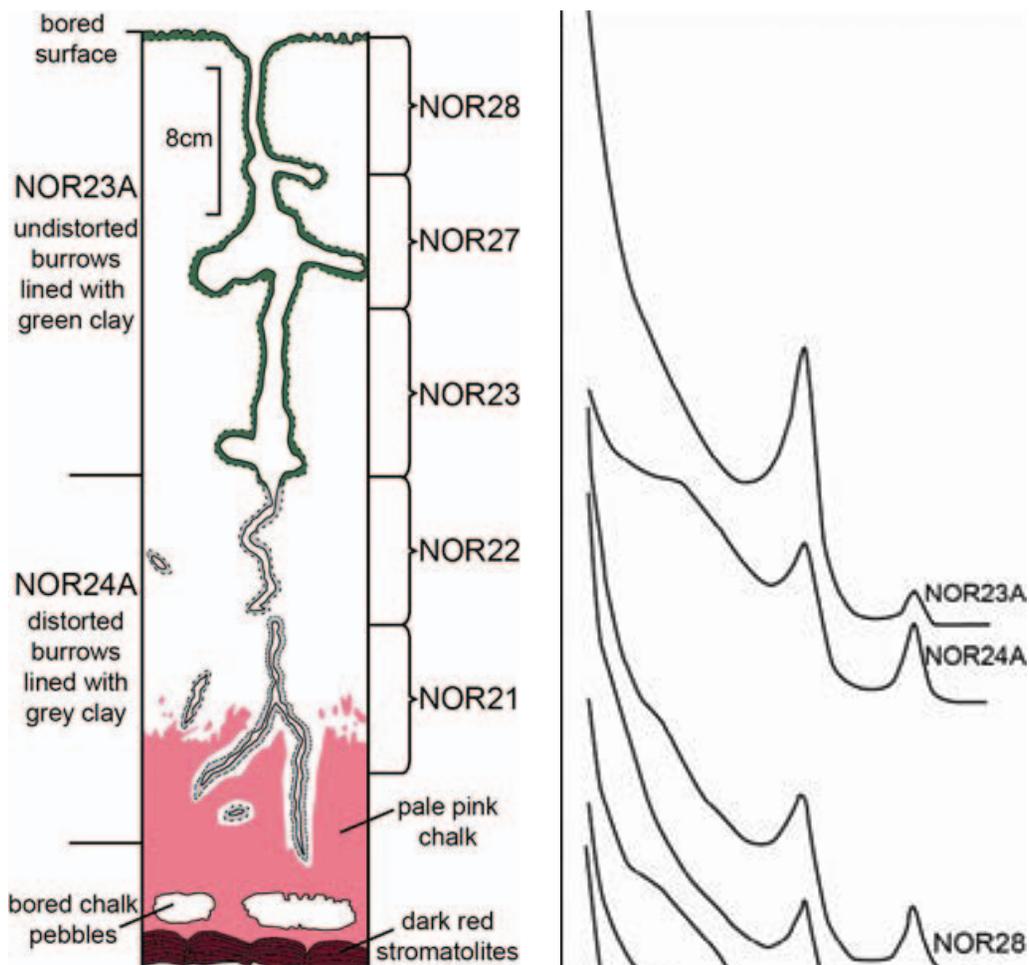
FIG. 8. Schematic section through the Paradoxica Bed at Hunstanton showing the distribution of samples.

single grain population centred at 0.17 μm for NOR21-23 and NOR24A, and at 0.49 μm for NOR27 and NOR28. The green clay burrow lining (NOR23A) has two grain populations, one centred at 0.49 μm (similar to NOR27–28) and the other at

FIG. 9. XRD patterns of the 400ºC heated <0.2 μm e.s.d. fractions of the Hunstanton samples showing the different degrees of collapse of the smectite peak. Samples NOR21–28 are from the main body of the Paradoxica Bed and arranged in stratigraphical order from bottom to top. Sample NOR24A is the grey clay burrow lining. Sample NOR23A is the green clay burrow lining.
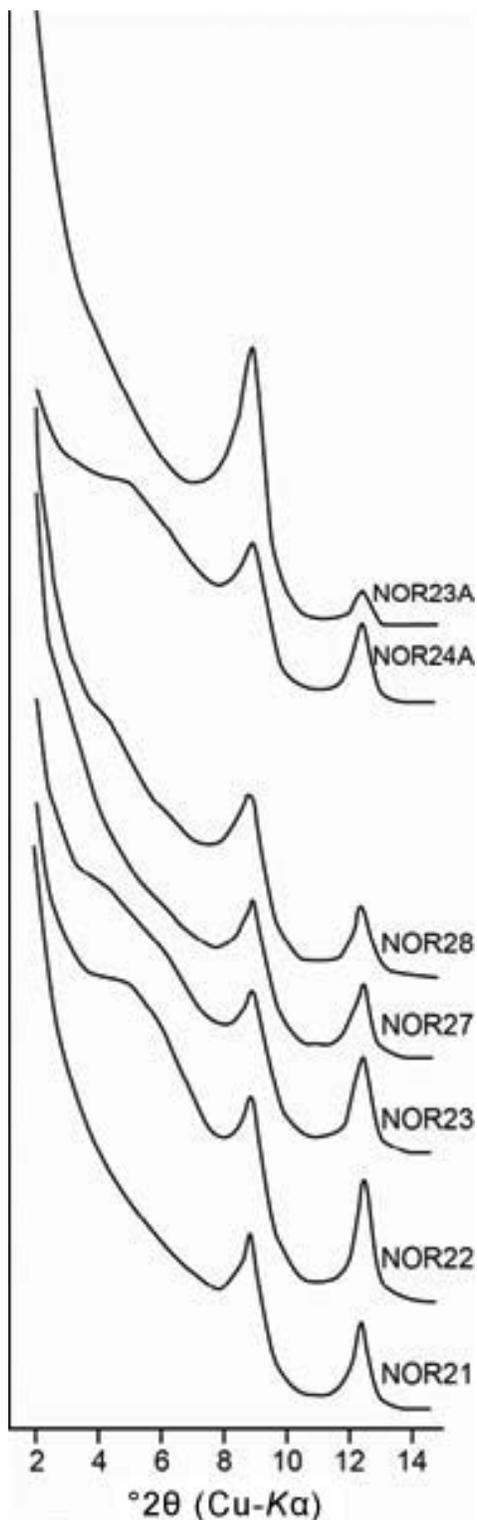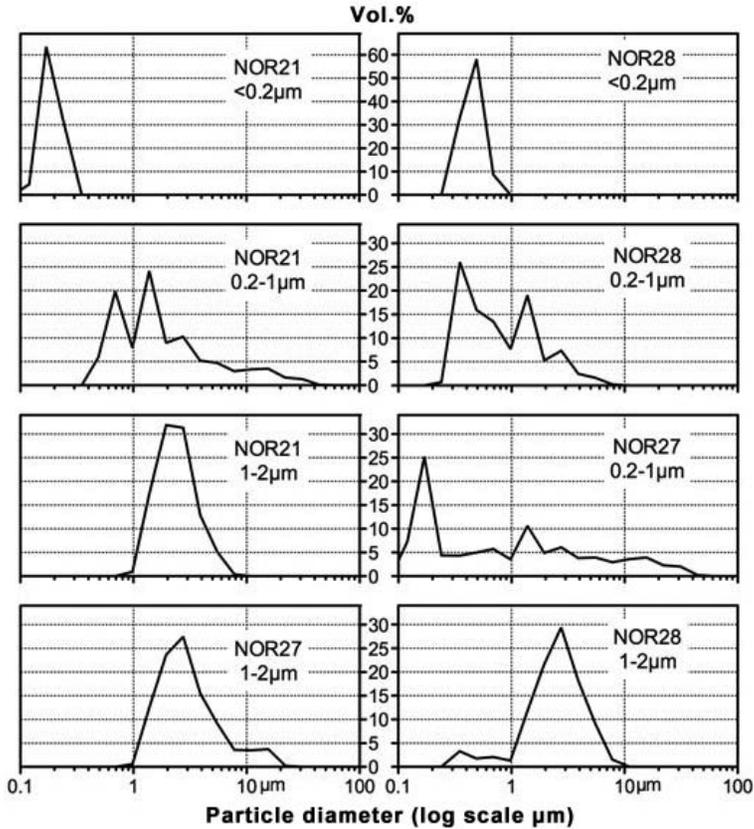
FIG. 10. Mastersizer particle size distribution patterns of the <0.2 μm e.s.d., 0.2−1 μm e.s.d. and 1−2 μm e.s.d. fractions from the Paradoxica Bed, Hunstanton. NOR21 is from the base of the bed, and NOR27 and NOR28 are from the top.

1.4 μm with a shoulder at 2.8 μm and a substantial tail to 5.5 μm.

The 0.2−1 μm e.s.d. fractions of NOR21–23 (Fig. 10) are similar, with pronounced grain populations at 0.69 μm and at 1.38 μm with a long tail to larger size particles. The uppermost two samples, NOR27–28, have their major grain populations at below 1 μm, centred at 0.17 μm for NOR27 and at 0.35 μm for NOR28 (Fig. 10); relative to NOR21–23 the proportion of larger particles is considerably reduced. The particle size distribution patterns of the two burrow linings are quite different (Fig. 11). NOR24A is similar to NOR21–23 but the relative size of the population centred at 0.69 μm has decreased and those at 1.38 μm and ≥1.95 μm have increased. The pattern shown by the green clay burrow lining, NOR23A, displays a great increase in the proportion of >1.38 μm grains, little evidence of well defined

individual populations, with a broad dominant grain population ranging from 2.76 to 5.5 μm.

All samples except for NOR23A provided 1−2 μm e.s.d. fractions. NOR21-23 show well defined grain populations centred at 2.0 and 2.8 μm with a tail to larger sizes including a small but distinctive 5.5 μm particle population (Fig. 10). Samples NOR24A (grey clayey burrow lining) and the top two samples (NOR27–28) are dominated by a population centred at 2.8 μm (Figs 10 and 11). In NOR27 the 2.8 μm population has a slight shoulder at 2 μm and a pronounced one between 11 and 16 μm.

Large ammonites from the Chalk at Speeton, Yorkshire

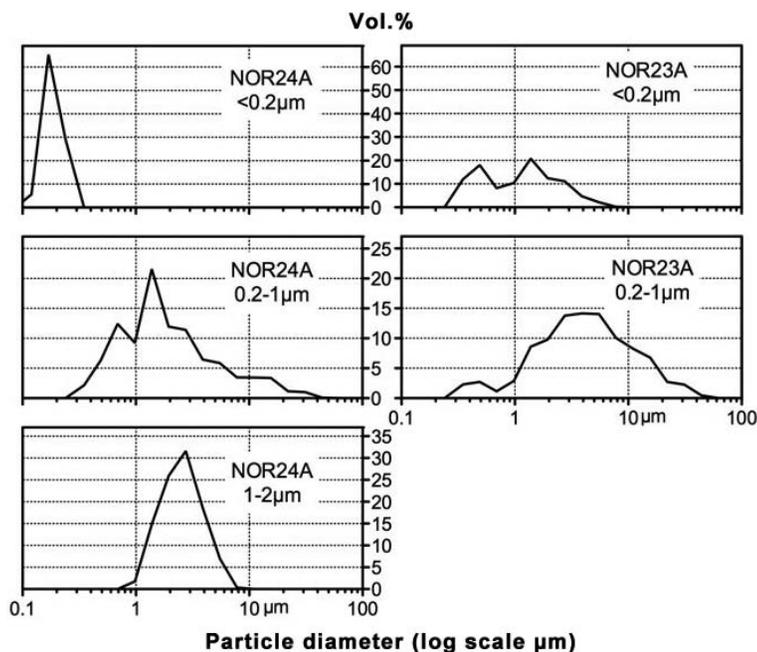The chalk infilling and underlying large ammonites is typically affected by early cementation and

Fig. 11. Mastersizer particle size distribution patterns of the <0.2 μm e.s.d., 0.2−1 μm e.s.d. and 1−2 μm e.s.d. fractions from the Paradoxica Bed, Hunstanton. NOR24A is from the grey clay burrow lining. NOR23A is from the green clay burrow lining.

lithification (Jeans, 1980, p. 116) and may contain the fossil traces of originally aragonite-shelled organisms that are rarely preserved in normal chalk (Wright, 1935). Three large ammonites, A1−A3 from the Lower and Middle Cenomanian part of the Ferriby Formation at Speeton have been investigated, their precise stratigraphical location is shown in Jeans (1980, fig. 16).

Volume and chemistry of calcite cement. The ammonite chalk has higher bulk density and $CaCO_3$ contents and a lower porosity than the nodules of the nodular chalk that surround them (Jeans, 1980, p. 116). Porosities range from 3.9 to 11.4% compared to 6.7 to 12.8% for the nodules. Comparison with the **Standard Louth Chalk** suggest cement values ranging from 28.6 to 36.1%, but these are minimum values as lithification set in prior to the completion of primary compaction.

Bulk calcite analyses show that the ammonite chalk has enhanced values of Mg, Mn and Fe relative to the matrix of their surrounding chalk (Jeans, 1980, table 8: Hu *et al.*, 2014, table 1). This pattern of trace element enhancement is comparable to the suboxic cement series recorded in the

terebratulid brachiopods from the Ferriby Formation of eastern England by Hu *et al.* (2012).

Clay mineralogy. The clay mineral analysis of the <0.2 μm and 0.2−1 μm fractions from the three ammonites and the surrounding nodular chalk are given in Table 4. The clay mineralogy of the ammonites and the nodular chalks is similar. The <0.2 μm fraction is dominated by dioctahedral smectite (97−100%) with traces of mica (up to 3%), and kaolinite. The 0.2−1 μm fraction has a slightly lower content of smectite (86−97%) with minor mica (2−8%) and kaolinite (1−8%) and traces of chlorite occur in one sample. None of the samples provided sufficient 1−2 μm fraction for XRD analysis. No systematic variations were noted in the degree of collapse of the 001 peak of the <0.2 μm dioctahedral smectite in the ammonite and its surrounding nodular chalk on heating to 400ºC.

Particle size distribution patterns. These are similar for all three ammonites. Figure 12 shows the pattern for Ammonite A1. The patterns for the <0.2 μm e.s.d. and 0.2−1 μm e.s.d. fractions have grain populations centred at ~0.2 μm and 1.1−1.2 μm. The one at ~0.2 μm dominates in the <0.2 μm e.s.d. fraction whereas the ~0.2 μm and the

TABLE 4. Clay mineralogy of chalk associated with large ammonites from the Ferriby Formation at Speeton, Yorkshire, UK.

Ammonite no.	Sample	Size fraction (μm)	Smectite (%)	Mica (%)	Kaolinite (%)	Chlorite (%)
A!	AI*	<0.2	100	tr	tr	—
	NI*	<0.2	100	tr	tr	—
	matrix	<0.2	100	tr	tr	tr
A3	AI	<0.2	98	2	tr	—
	NI	<0.2	100	tr	tr	—
	matrix	<0.2	100	tr	tr	—
A4	AI	<0.2	100	tr	tr	—
	NI	<0.2	100	tr	tr	—
	matrix	<0.2	97	3	tr	—
A1	AI	0.2 to 1	97	2	1	—
	NI	0.2 to 1	80	12	8	—
	matrix	0.2 to 1	86	8.5	5.5	tr
A3	AI	0.2 to 1	89	7	4	—
	NI	0.2 to 1	88	8	4	—
	matrix	0.2 to 1	88	7	5	—
A4	AI	0.2 to 1	97	2	1	tr
	NI	0.2 to 1	91	5	4	tr
	matrix	0.2 to 1	86	8.5	5.5	tr

AI ammonite interior
NI nodule interior

1.1−1.2 μm modes are of equal importance in the 0.2−1 μm fraction.

Nodular chalk at Speeton, Yorkshire

Nodular chalk is widespread in the Upper Cretaceous Chalk of the UK. It is a diagenetic facies caused by localized centres of calcite cementation prior to the completion of primary compaction. This results in a lithology of harder nodules up to fist size set in a matrix of softer chalk or marly chalk. When this facies has developed in red or pink coloured chalks, the nodules and their acid insoluble residues are always paler in colour than the matrix and its acid insoluble residue (Jeans, 1980, p. 121, see Type-5 lithification; Hu *et al.*, 2014, fig. 8). Five nodular chalks (F3, F5–7, F10) from the Lower and Middle Cenomanian part of the Ferriby Formation at Speeton have been investigated. Their stratigraphical location is shown in fig. 5 of Hu *et al.* (2014).

Volume and chemistry of calcite cement. Nodule porosities measured in the Ferriby Formation at Speeton range from 6.7 to 14.8% with the most values between 10 and 14% (Jeans, 1980, table 9). Comparison with the **Standard Louth Chalk** suggests cement volumes of 25 to 33%; these are minimum values as lithification and cementation were initiated before the completion of primary compaction. The trace element chemistry of the bulk calcite is characterized by the enhanced Fe content of the nodules relative to the matrix, in some instances by a factor of 2 to 3 times (Jeans, 1980, table 10; Hu *et al.*, 2014, table 2). The cement responsible for the nodules is enriched in Fe and is considered equivalent to the Fe-rich phase of the suboxic cement series identified by Hu *et al.* (2012).

Clay mineralogy. The clay mineral analysis of the <0.2 μm, 0.2−1 μm and 1−2 μm fractions are given in Table 5. The <0.2 μm fraction of both nodules and matrices are dominated by dioctahedral smectite (89−100%) with minor amounts of mica

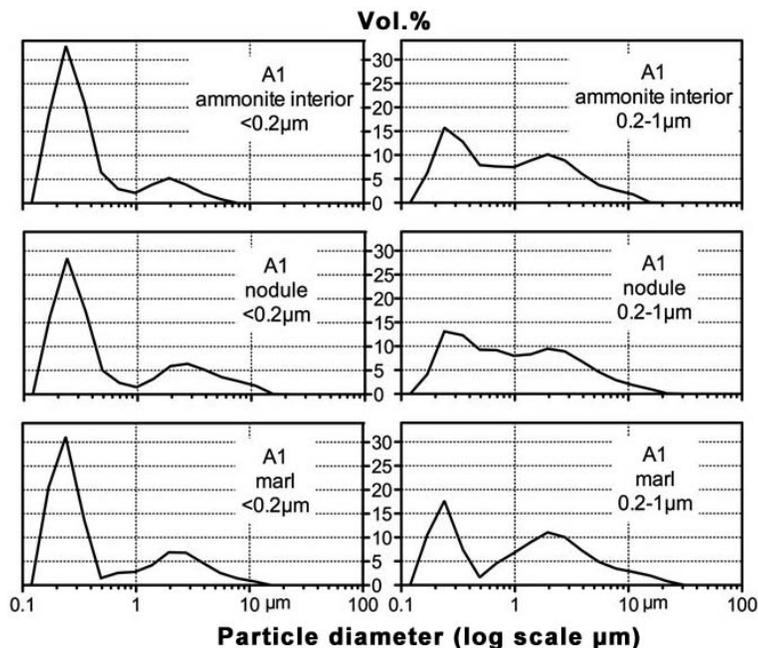Fig. 12. Mastersizer particle size distribution patterns of the <0.2 μm e.s.d. and 0.2−1 μm e.s.d. fractions from large ammonite (A1) and its nodular chalk surrounds, Ferriby Formation, Speeton.

(trace−5%), berthierine (trace−2%) with occasional traces of kaolinite. In the 0.2−1 μm fraction the smectite content (38−67%) is reduced, whereas mica (22−33%), kaolinite (trace−37%) and berthierine (trace−15%) are enhanced − traces of chlorite are also present. Analyses of the 1−2 μm fractions are only available for the matrices of F6 and F7, and the nodule of F10. The 1−2 μm clay mineralogy of the matrices of F6 and F7 are dominated by smectite (94−98%) with minor or trace amounts of mica, kaolinite, berthierine and chlorite − an assemblage very similar to the <0.2 μm fraction. The 1−2 μm fraction of the nodules from F10 is dominated by smectite with minor mica and a trace of kaolinite.

Systematic differences occur in the degree of collapse on 400ºC heating shown by the 001 smectite peak from the <0.2 μm fraction of corresponding nodules and matrices. Figure 13 shows that in each nodular chalk the smectite of the nodules displays more resistance to collapse than the smectite from their matrices.

Particle size distribution patterns. There was insufficient material to carry out particle size analyses on the separated <0.2 μm e.s.d., 0.2−1 μm e.s.d. and 1−2 μm e.s.d. fractions.

Regionally hardened chalk at Speeton, Yorkshire

The upper half of the Louth Member, Ferriby Formation, is of Upper Cenomanian age. It has been regionally cemented, showing little or no field evidence of early lithification. Modelling of the geochemical pattern of its calcite cementation suggests that it involved two phases. The first was under considerable overpressure with the precipitation of calcite cement displaying the chaotic geochemical patterns (Hu *et al.*, 2012) under conditions little different from those of early lithification except that (1) cementation was not localized but widespread, (2) deposition rates were higher, and (3) there was considerable overpressure. The second phase was triggered by the loss of overpressure resulting in greatly increased grain pressure causing grain welding, pressure dissolution and the development of stylolites with the concentrations of the acid insoluble residues from the adjacent chalk. This second phase is responsible for the lithification of the chalk and the subsequent development of brittle fracture. It is also associated with the penetration of allochothonous porefluids, possibly from the North Sea Basin, into the Chalk.

TABLE 5. Clay mineralogy of nodular chalk from the Ferriby Formation at Speeton, Yorkshire, UK.

Sample	Size fraction (μm)	Smectite (%)	Mica (%)	Kaolinite (%)	Berthierine (%)	Chlorite (%)
F3 matrix	<0.2	100	tr	tr	–	–
F3 NI*	<0.2	100	tr	tr	–	–
F5 matrix	<0.2	89	3	8	–	–
F5 NI	<0.2	91	2	7	–	–
F6 matrix	<0.2	100	tr	tr	–	–
F6 NI	<0.2	100	tr	tr	–	–
F7 matrix	<0.2	100	tr	–	tr	–
F7 NI	<0.2	100	tr	–	tr	–
F10 matrix	<0.2	93	5	–	2	–
F10 NI	<0.2	100	tr	–	tr	–
F3 matrix	0.2 to 1	57	29	14	tr	tr
F3 NI	0.2 to 1	67	22	5.5	5.5	tr
F5 matrix	0.2 to 1	38	25	37	tr	tr
F5 NI	0.2 to 1	38	25	26	11	tr
F6 matrix	0.2 to 1	57	29	10	4	tr
F6 NI	0.2 to 1	45	28	13.5	13.5	tr
F7 matrix	0.2 to 1	63	25	6	6	tr
F7 NI	0.2 to 1	50	33	15	2	tr
F10 matrix	0.2 to 1	45	28	13.5	13.5	tr
F10 NI	0.2 to 1	54	31	tr	15	–
F6 matrix	1 to 2	94	4	2	tr	tr
F7 matrix	1 to 2	98	2	tr	tr	–
F10 NI	1 to 2	89	11	tr	–	–

NI nodule interior

Comparison is made between the clay mineralogy of five chalk samples and their associated clay-rich styolitic marl seams. Details of the sample locations are shown in Hu *et al.* (2014, fig. 5).

Volume and chemistry of calcite cement. The bulk density of the chalk samples range from 2.19 to 2.27 with porosities of 19 to 17%. Comparison with the **Standard Louth Chalk** suggests the cement volume ranges from 21 to 23%. Modelling of the trace element content of the calcite cement indicate that Fe averages 1500 ppm, Mn 1950 ppm, Mg 2400 ppm and Sr 730 ppm. There is a marked difference in stable isotope values between the calcite of the chalks and marl seams. The O^{16}/O^{18} values for the chalk range from −4.30‰ to −4.75‰, the C^{12}/C^{13} from 2.92‰ to 3.05‰. For the marls the O^{16}/O^{18} values are from −2.09% to −3.67% and the C^{12}/C^{13} values are from 3.07 to 3.18‰. The differences in stable isotope values between chalks and marl seams reflect the cementation of the chalk at enhanced temperatures and the contribution made by the relatively low C^{12}/C^{13} values of coccolith material undergoing preferential dissolution during the development of stylolites and marl seams to the C^{12}/C^{13} values of the calcite cement of the chalks (Jeans *et al.*, 2012).

Clay mineralogy. The clay mineral analysis of the <0.2 μm, 0.2−1 μm and 1−2 μm fractions are given in Table 6. There are subtle differences between the chalks and marl seams. In the <0.2 μm fraction, chalks have a slightly higher average content of dioctahedral smectite (90−100%, cf 80−95%) and a lower content of mica (trace, cf trace−7%). There is an absence of kaolinite and berthierine from the chalk but these are present in trace amounts in the marl seams. In the 0.2−1 μm fraction there is little difference between the chalks and marl seams, except for the presence of traces of chlorite in the marl seams. All the marl seams provided 1−2 μm fractions for XRD analysis, whereas only one chalk sample (R8) provided equivalent XRD data. If R8 is representative of the chalk samples, the analysis is similar to the general clay mineralogy of the marl seams
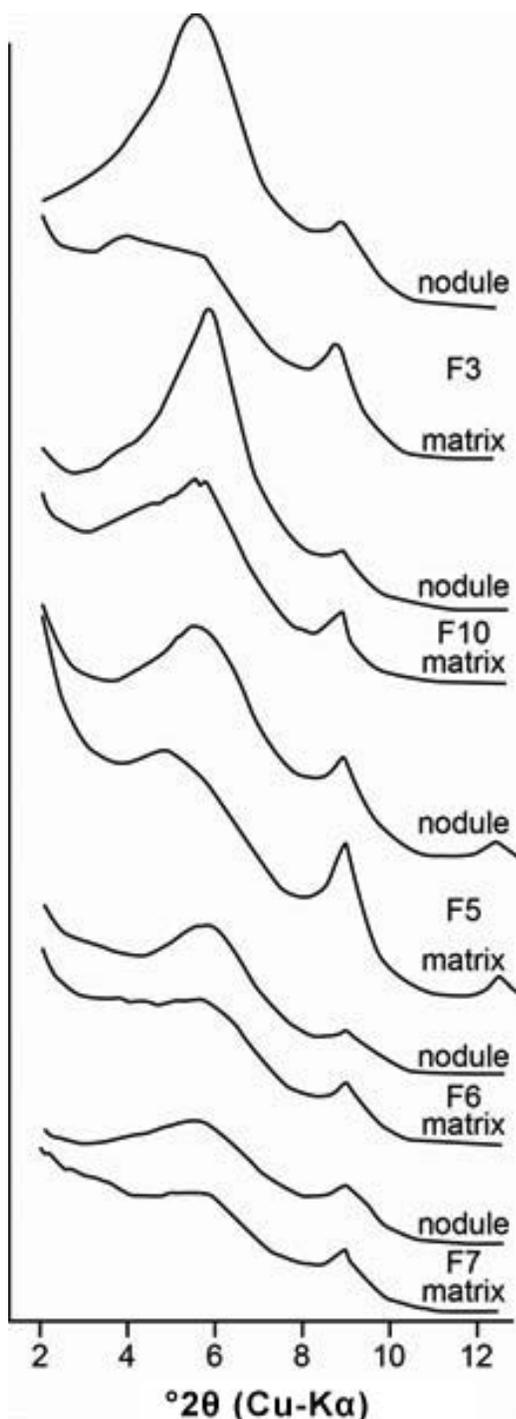
FIG. 13. XRD patterns of the 400ºC heated <0.2 μm
e.s.d. fraction showing the different degrees of collapse
of the smectite peak shown by the nodules and their
matrices of nodular chalks, Speeton, Yorkshire.

except that it does not contain the trace or minor
amounts of kaolinite and berthierine. There is
considerable range in the resistance to collapse of
the 001 peak of the dioctahedral smectite on 400ºC
heating exhibited in the <0.2 μm fractions from the
chalk and marl seams. No systematic pattern has
been observed. Figure 14 shows the range of
variation for the chalk samples.

Particle size distribution patterns. The patterns
for the <0.2 μm e.s.d., 0.2−1 μm e.s.d.and 1−2 μm
e.s.d. fractions and the total acid insoluble residues
of the chalks and marl seams are clearly
differentiated. Figure 15 contrasts the patterns
from typical samples.

In the total acid insoluble residues the marl seams
are represented by a broad grain population
stretching from 0.7 μm to 20 μm with the dominant
size at 2−4 μm and displaying a shoulder at
1.05−1.1 μm. The total acid-insoluble residue from
the chalks shows a greater range of particle sizes,
from 0.15 to 40 μm. The dominant particle size is
~3 μm with a distinct shoulder at 1.05−1.1 μm; there
is a distinct population in the 0.3−0.4 μm size range.

The <0.2 μm e.s.d. fractions from both the chalks
and marl seams have a well defined grain
population centred at 0.15 μm with a shoulder at
~0.09 μm. The marl seams have grain populations
in the 2.0−2.8 μm and 16−22 μm size ranges
which are either absent or hardly discernible in the
chalks. The 0.2−1 μm e.s.d. fractions of the chalks
and marl seams are similar. They contain two grain
populations, a well-defined one centred at 0.15 μm
and a broad one extending from 0.4 μm to about
8−11 μm. The 1−2 μm fraction of the marl seams
have grain populations with a sharply defined minor
one centred at 0.25 μm and a major one at 2−3 μm.
There are no data from the chalk samples.

DETAILED INTERPRETATION

Heat stability of dioctahedral smectite

Variations in the dehydroxylation temperatures of
different smectites and mixed layer I/S are well
established, particularly the lower temperatures
displayed by dioctahedral compared to trioctahedral
types (e.g. Mackenzie, 1970). Mackenzie (1972) has
suggested that there is a connection between the
heating behaviour and chemical composition. More
recently a better understanding of the octahedral
layer and its different cation sites and their
occupancy in dioctahedral smectites has provided

TABLE 6. Clay mineralogy of the regionally hardened chalk in the Louth Member of the Ferriby Formation at Speeton, Yorkshire, UK.

Sample	Size fraction (μm)	Smectite (%)	Mica (%)	Kaolinite (%)	Berthierine (%)	Chlorite (%)
R6	<0.2	100	Tr	–	–	–
R8	<0.2	100	Tr	–	–	–
R9	<0.2	100	Tr	–	–	–
R12	<0.2	100	tr	–	–	–
R13	<0.2	100	tr	–	–	–
R6	0.2 to 1	73	18	9	–	–
R8	0.2 to 1	81	11	8	–	–
R9	0.2 to 1	79	14	7	–	–
R12	0.2 to 1	83	10	7	–	–
R13	0.2 to 1	86	8	6	–	–
R8	1 to 2	78	20	2	–	–
YSA34	<0.2	93	7	tr	tr	–
YSA36	<0.2	97	3	tr	tr	–
YSA45	<0.2	97	3	tr	tr	–
YSA47	<0.2	97	3	tr	tr	–
YSA48	<0.2	100	tr	tr	tr	–
YSA34	0.2 to 1	81	13	6	–	tr
YSA36	0.2 to 1	81	13	6	–	tr
YSA45	0.2 to 1	87	10	3	–	–
YSA47	0.2 to 1	84	12	4	–	–
YSA48	0.2 to 1	88	9	3	–	–
YSA34	1 to 2	40	33	20	–	7
YSA36	1 to 2	33	38	21	–	8
YSA45	1 to 2	56	31	13	tr	tr
YSA47	1 to 2	72	20	8	–	tr
YSA48	1 to 2	72	20	8	tr	tr

a basis upon which the pattern of dehydroxylation can be used as a proxy for chemical composition (Brigatti, 1983; Kawano & Tomita, 1991; Drits & McCarty, 1996; Wolters & Emmerich, 2007; Wolters *et al.*, 2009). Brigatti (1983) showed that there is good correlation between the dehydroxylation peak temperature, the Fe content and *b* dimension of the unit cell in the montmorillonite-nontronite series, with the increasing Fe content being associated with lower dehydroxylation temperatures. With an increasing amount of Fe there is a parallel increase in the proportion of trans-vacant sites relative to cis-vacant sites which dominate beidellitic and montmorillonitic dioctahedral smectites (Wolters *et al.*, 2009).

At this stage of our investigation the clay assemblages were not subjected to analysis by differential thermal or differential thermal gravimetric methods. However we were particularly interested to observe how variable were the degrees of collapse on 400ºC and 550ºC heating shown by dioctahedral and possibly trioctahedral smectites from different cementation settings. Our hypothesis was that a relatively increased resistance to collapse indicates a dehydroxylation peak at a higher temperature, which might suggest a lower Fe and a higher Mg or Al occupancy in the octahedral layer. Systematic correlation would provide support for carrying out a more detailed investigation in the future. Examination of the diffractograms from the 101 separated fractions from our 42 samples reveals general relationships regarding the resistance of smectite to 400ºC and 500ºC heating. The 001 peak of smectite in every fraction in which these
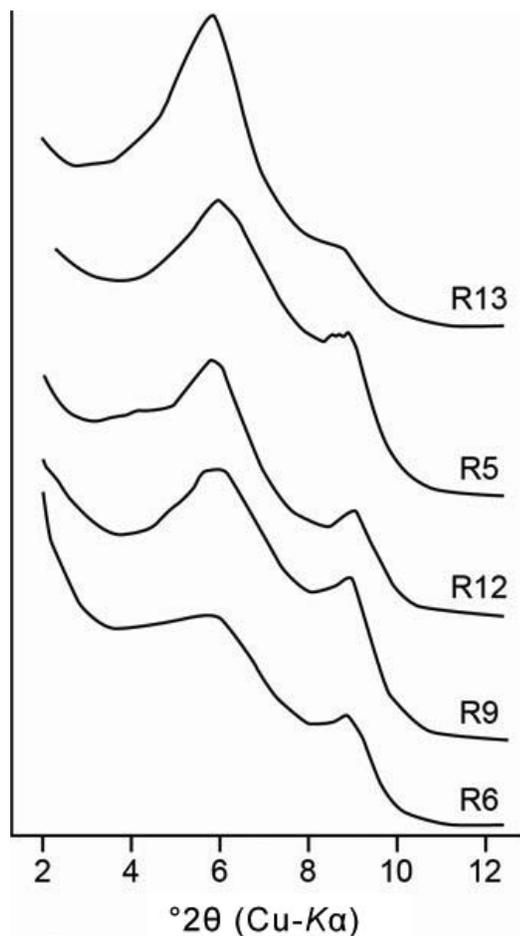
C. V. Jeans et al.

FIG. 14. XRD patterns of the 400ºC heated <0.2 μm e.s.d. fractions showing the different degrees of collapse of the smectite peak in chalk samples from the regionally hardened chalk of the Ferriby Formation (Louth Member), Speeton, Yorkshire.

samples that show 400ºC resistance display a distinct pattern within their different particle size fractions in which greatest resistance is shown by the <0.2 μm fraction followed by lower or an absence of resistance in the 0.2−1 μm fraction. If a 1−2 μm fraction is present (only 17 samples have 1−2 μm fractions) it shows typically no resistance (Fig. 16). Three samples (F6 matrix, F7 matrix, F10 nodule) show a different pattern with the greatest resistance in the 1−2 μm fraction (Fig. 17). Systematic differences in samples from a particular variety of lithification are developed only in the nodular chalks (Fig. 13). Here the dioctahedral smectite of the <0.2 μm fraction from the nodules is more heat resistant than in the adjacent marly matrix. This suggests that Fe available in the porefluids within the nodules preferentially entered the calcite cement depleting the pore waters of Fe, resulting in the neoformation of Fe-poor dioctahedral smectite. Comparison between smectite in the different types of lithification and the resistance to collapse shows that the most resistant are associated with the ammonite chalk, the nodular chalk and the regionally hardened chalk at Speeton, whereas the samples from Hunstanton and Peacehaven have lower resistance. The hardground samples from Hunstanton display particularly low resistance and this could be related to the exceptionally early cementation of the Paradoxica Bed or perhaps more likely to the enhanced Fe concentrations in the porefluids that could arise from the dissolution of any Fe oxide /hydroxide that may have been present in the original sediment.

Particle separates and particle size distribution patterns

The separation of the <0.2 μm e.s.d., 0.2−1 μm e.s.d. and 1−2 μm e.s.d. fractions has been based upon sedimentation rates applying Stokes formula either under normal or centrifugally enhanced gravitation. The total depositional distance used to segregate particle size fractions ranged for 45 cm to ~85 cm with no attempt being made to completely remove smaller grain sizes outside the prescribed range. It is only the <0.2 μm e.s.d. fraction that should have no particles outside its prescribed range, whereas the 0.2−1 μm e.s.d. should contain no particle larger than 1 μm e.s.d. but is likely to contain particles of <0.2 μm e.s.d.. Similarly the 1−2 μm e.s.d. fraction may contain some <1 μm e.s.d. particles but it should not contain particles larger than 2 μm e.s.d..

minerals occur shows some degree of collapse on 400ºC heating and complete collapse in 550ºC heating. Only four samples, all from Hunstanton, display complete or practically complete collapse on 400ºC heating (Fig. 9). We have tentatively interpreted this range of resistance to represent either (1) variations in the relative proportions of an Fe-rich (no resistance) and a relatively Al-rich (resistant) smectite mineral, or (2) smectite with a variable or particular Al/Fe composition, or (3) a combination of (1) and (2). Some of this variation in collapse could be related to rehydration after heating but this is considered unlikely as the heating times were 2 h (Greene-Kelly, 1957). The majority of

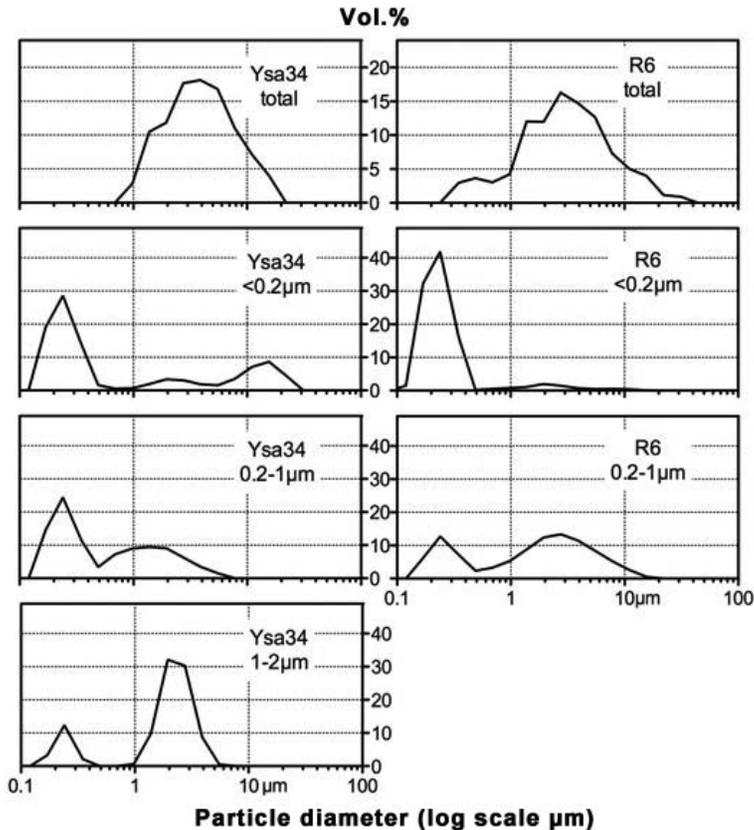FIG. 15. Mastersizer particle size distribution patterns of the total acid insoluble fracton and the <0.2 μm e.s.d., 0.2−1 μm e.s.d. and 1−2 μm e.s.d. fractions from typical samples of chalk (R6) and marl seam (Ysa34) from the regionally hardened chalk, Ferriby Formation (Louth Member), Speeton, Yorkshire.

As stated earlier the Malvern Mastersizer 2000 estimates particle size by measuring the intensity of light scattered as a laser beam passes through the dispersed particulate sample. For fully dispersed suspensions of particles of the same shape and density the method will record larger diameter particles than gravitation settling methods. The extent of the difference is related to the shape of the particles; with increasing aspect ratios of the particles the larger will be the difference. The particle size distribution patterns of the <0.2 μm e.s.d., 0.2−1 μm e.s.d. and 1−2 μm e.s.d. fractions that we have recorded from the various types of lithification fall into two groups. The first consists of the fractions from the chalk at Peacehaven and Speeton which are dominated by smectite. The second group are the samples from Hunstanton and these contain mica and kaolinite as major components in addition to smectite.

Particle size fractions from Peacehaven(Figs 6, 7) and Speeton (Figs 12 and 15). The <0.2 μm e.s.d. fractions are dominated by a large particle population ranging from 0.1 to 0.5 μm with the majority at 0.2−0.25 μm. In some samples there is in addition a minor poorly defined particle population ranging from 0.4 to 14 μm. The dominant population (0.1−0.5 μm) can be matched with the expected gravitation separation (<0.2 μm) whereas the 0.4 to 14 μm population cannot. These larger grains recorded by the laser diffraction method are interpreted as groups of loosely flocculated small particles with sedimentation rates little different than the finest particles. This suggests that the <0.2 μm e.s.d. fraction is made up of two groups of fine particles, one is flocculated, whereas the majority are in a dispersed state.

In the 0.2−1 μm e.s.d. fractions, the 0.1−0.5 μm population is much reduced and represents the
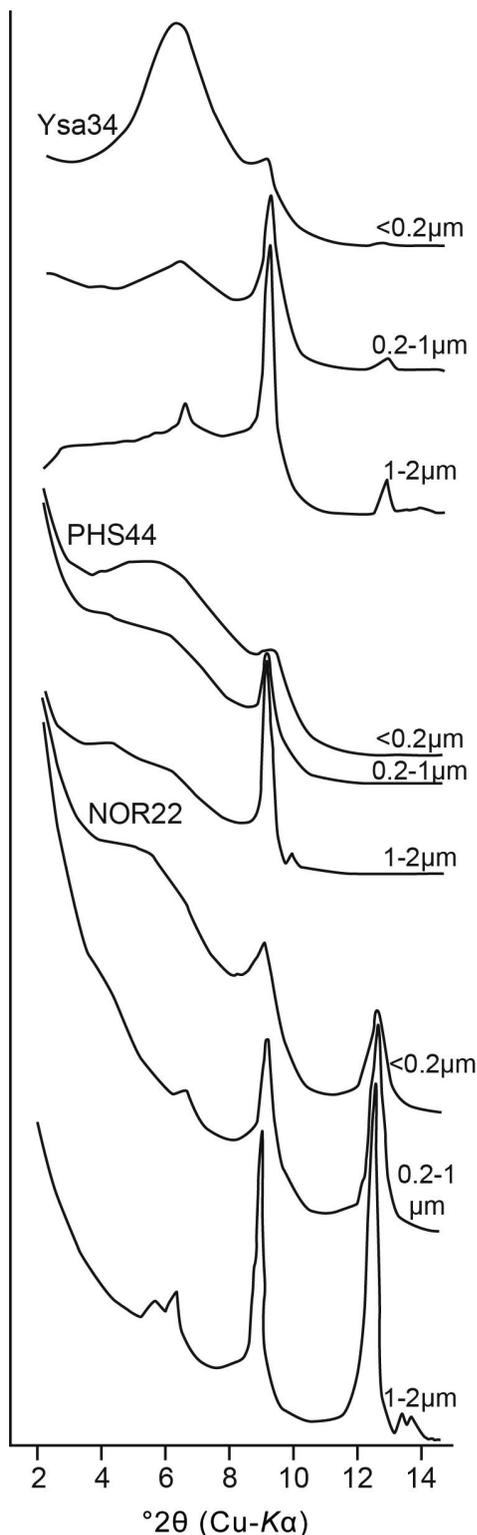
unflocculated grains in the <0.2 μm e.s.d. fraction that were not removed during gravitational settling. The 0.4−14 μm grain population dominates and this is interpreted as floccules of low surface charge smectite mixed with talc, mica or kaolin as minor components.

In the 1−2 μm e.s.d. fraction, a small residual 0.1−0.5 μm population is still present reflecting inadequate separation, whereas the fraction is dominated by particles between 1 and 10 μm. The range of particle size is reduced compared to the 0.2−1 μm e.s.d. fraction with the majority varying between 2 and 7 μm, we suggest that this predominant population consists mainly of separate unflocculated grains.

Particle size fractions from Hunstanton (Figs 10 and 11). These fractions have clay assemblages consisting of dioctahedral smectite, mica and kaolinite as major components. Their <0.2 μm e.s.d. fractions have a single grain population centred at 0.2 μm or 0.4 μm representing dispersed particles. There is no evidence of the large flocculated grains typical of the samples from Peacehaven.

The 0.2−1 μm e.s.d. fractions are characterized by the presence of particle populations that may or may not be represented in the <0.2 μm e.s.d. fraction. In NOR21 there are new populations at 0.7 μm, 1.5 μm and 2.8 μm (Fig. 10) which are present to a greater or lesser extent in all samples except for NOR23A, the green clay lining of the burrows. All the 0.2−1 μm e.s.d. fractions have a long tail of large particles extending from 4 up to 30 or 40 μm which are interpreted as large floccules. The 0.2−1 μm e.s.d. particle distribution pattern in NOR27 is exceptional with particles ranging from 0.1 to 30 μm; there is a major population at 0.17 μm (unrepresented in any of its size fraction but typical of the <0.2 μm e.s.d. fraction in NOR21-23) with evidence of particle populations of 0.7 μm, 1.5 μm and 2.8 μm. A possible explanation is that this fraction was flocculated when collected − and that during particle size analysis it redispersed into a mixed <0.2 μm/0.2−1 μm e.s.d. suspension. If this is the case it could suggest that the 0.49 μm particles of

FIG. 16. XRD patterns of the 400ºC heated <0.2 μm e.s.d., 0.2−1 μm e.s.d. and 1−2 μm e.s.d. fractions showing typical degrees of collapse of the smectite peaks in relation to grain size exhibited by most samples in this study.
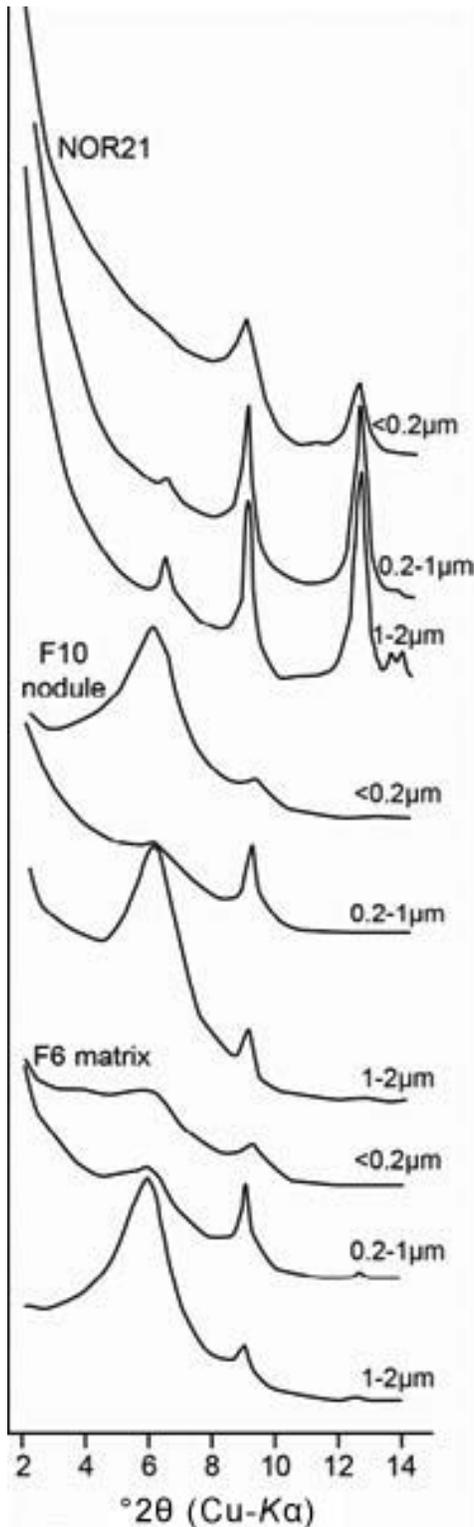
the <0.2 μm e.s.d. fraction were actually floccules of even finer particles.

The 1−2 μm e.s.d. fractions consist predominantly of particles between 1 and 10 μm dominated by those between 2 and 3 μm. Some samples have small residual particle populations representing the <1 μm material as well as the flocculated >10 μm grains.

GENERAL INTERPRETATION

Each of the five types of chalk lithification displays a different association between the mineralogy and particle size distribution pattern of its clay mineralogy and the timing and geochemistry of the calcite cementation. An important question is the extent to which these associations reflect either different stages in the diagenetic development of the chalk's clay mineral assemblage or just regional and stratigraphical differences in the detrital clay mineral assemblage entering the Chalk Sea. The significance of the variation in the laser-based particle size distribution patterns is not clear. There is some correlation with the general composition of the clay assemblage, whether it is from a more distal facies (kaolinite absent) or more proximal one (kaolinite present). The role of the cementation process and the structure of the pore system in moulding crystal size, shape and form is not clear; however the general similarity in particle size patterns between the slightly and the extensively cemented chalk samples from, respectively, Peacehaven and Speeton suggest that this influence is limited.

Although these questions cannot be attempted without a more extensive survey of similar lithification types at new horizons and locations, various aspects of our findings pertinent to this will be discussed.

Regional and stratigraphical factors

The main part of the Chalk (Turonian−Early Maastrichtian) in the UK contains a very low acid-

FIG. 17. XRD patterns of the 400ºC heated <0.2 μm e.s.d., 0.2−1μm e.s.d. and 1−2 μm e.s.d. fractions showing the range of variation in the degree of collapse of the smectite peak in relation to grain size exhibited by NOR21 (complete collapse), F10 nodule (enhanced resistance in the <0.2 μm e.s.d. and 1−2 μm e.s.d. fractions) and F6 matrix (enhanced resistance in the 1−2 μm e.s.d. fraction).

insoluble residue characterized by a clay mineral assemblage dominated by smectite and minor mica. The lowest part of the Chalk (Cenomanian) typically contains a higher acid-insoluble residue and it displays a more varied clay mineral assemblage which may contain considerable proportions of kaolinite, mica and smectite. The clay assemblages from Peacehaven come from the main part of Chalk, and we considered them to be little different to those from the Cenomanian Chalk at Speeton except for their lower acid insoluble residue. However our more detailed analysis demonstrates that there are significant differences. The collapsible mineral at Peacehaven is a mixture of dioctahedral smectite with some nontronite or trioctahedral smectite whereas at Speeton it is dioctahedral smectite. Kaolinite is completely absent from Peacehaven whereas it is an appreciable component of the $0.2-1$ μm e.s.d. and $1-2$ μm e.s.d. fractions at Speeton, linking these chalks with those rich in the kaolin-mica detrital assemblage such as occur in the Paradoxica Bed of Cenomanian age at Hunstanton. The predominant collapsible mineral in the Cenomanian Chalk of southern England is smectite as reported by Perrin (1964), Young (1965) and Jeans (1968). Our findings suggest that this dioctahedral smectite differs from the mixed dioctahedral smectite-nontronite/triocta-hedral smectite assemblage characteristic of the low acid-insoluble chalk at Peacehaven.

Trace elements in calcite cement

The entry of trace elements into the calcite cements responsible for Chalk lithification or into neoformed clay phases depends both upon their availability and the ease of their incorporation into the calcite or silicate structures. The availability of Mg^{2+} will depend on (1) its concentration in the porewaters, and (2) its replenishment from the overlying Chalk Sea as it is utilized in diagenetic reactions − this will be controlled by the rate of deposition (fast deposition with little chance for replenishment, slow or nil deposition ideal for replenishment). At Peacehaven calcite cementation seems to have set in at considerable depth below the water-sediment interface and is very low in Mg^{2+}. The possible presence of appreciable amounts of talc and trioctahedral smectite, assuming these are of neoformationed origin, suggests that the Mg was utilized at an earlier stage in clay-forming reactions. Contrasted with this

are the Mg-rich early diagenetic calcite cements associated with the Paradoxica Bed hardground at Hunstanton and the large ammonites at Speeton, both of which seemed to have mopped up any available Mg leaving nothing for clay mineral reactions.

The relative availability of Fe^{2+} for calcite- and clay-forming reactions was markedly different between the Cenomanian chalk of eastern England and the Campanian chalk at Peacehaven. At Speeton the conditions of intrinsic diagenesis never became anoxic. Ferric hydroxide, now preserved as a fine-grained hematite pigment, was widespread and is the colouring pigment in the red to very pale pink chalks. Some of this $Fe(OH)_3$, mobilized in the suboxic zone but not taking part in the precipitation of iron sulfides (Hu *et al.*, 2012), was available for incorporation in both calcite cements and neoformed clay minerals. At Peacehaven pink or red coloured chalks are absent. It was quite possible that ferric hydroxide was originally present but underwent anoxic diagenesis with the precipitation of iron sulfides leaving the porefluids low in Fe^{2+}, and this is reflected in its low concentration in the model cement. Regional evidence indicates that the Paradoxica Bed hardground at Hunstanton was developed in sediments that were originally rich in $Fe(OH)_3$. There is evidence that (a) anoxic conditions did develop during the main phase of calcite precipitation with the total dissolution of the $Fe(OH)_3$, and (b) part may have been precipitated as iron sulfide, but there was sufficient Fe in solution for it to be an appreciable trace element in the calcite cement as well as being involved with clay mineral neoformation not just in the green clay-rich zone coating the burrow walls but also within the main body of the bed.

Berthierine and chlorite occur either as a trace or minor component in many samples from eastern England (Hunstanton, Speeton) but have not been identified at Peacehaven. This regional pattern is probably related to the differing conditions of diagenesis with berthierine being associated with the extended period of suboxic diagenesis in eastern England where Fe was available in the porefluids and was not being taken up in sulfide precipitation. At Speeton, in the regionally hardened chalk, the restriction of kaolinite and traces of berthierine to the pressure dissolution marl seams and their absence from the chalk could be related to the invasion by allochthonous anoxic porefluids that

have been linked to the loss of overpressure, followed by lithification, then by the sulfidization of the red hematite pigment at various horizons in the Ferriby Formation.

Resistance to heating

The variable resistance of the smectite to 400ºC heating reflects at least in part a diagenetic feature related to the neoformation of the collapsible phase within the sediment and not to an inherited feature of a detrital clay phase. In the nodular chalks at Speeton, the <0.2 µm e.s.d.clay fractions show a general difference in the heat resistance between nodule and matrix which suggests that when there was competition between calcite and smectite-forming reactions, Fe entered preferentially the carbonate structure. On a regional scale the low heat resistance of the smectite at Hunstanton reflects the high availability of Fe^{2+} in the development of the Paradoxica Bed hardground and provides evidence for the extensive development of the collapsible phase during diagenesis.

CONCLUDING DISCUSSION

Particular attention has been given in Denmark (Lindgreen *et al.*, 2002, 2008; Drits *et al.*, 2004)) and France (Deconinck & Chamley, 1995) to the nature of the smectitic phases in the Chalk. In Denmark investigations have concentrated on the description and modelling of the mixed-layer phases; these occur in the Chalk at the surface and in offshore oil wells in the Danish sector of the North Sea where samples from depths in excess of 3000 m have been studied. Two main series have been identified, a *high-smectite/illite-smectite mixed-layer* (HS/I-S) with 95% smectite layers and a *low-smectite/illite-smectite mixed-layer* (LS/I-S) with 50% smectite layers. The *low-smectite/illite-smectite* series may also contain layers of chlorite (LS/I-S-Ch) or vermiculite (LS/I-S-V). A third series is based around chlorite; there is a mixed layer chlorite-serpentine (Ch 90%–Sr 10%) exhibiting euhedral crystals and a tosudite phase consisting of regular interlayered chlorite with smectite or vermiculite occurring as ribbon shaped crystals. The stratigraphical and depth distribution of these different mixed layer phases display no consistent pattern. There is geological evidence that these mixed layer phases were present within the Chalk prior to the phase of pressure

dissolution responsible for the stylolites and marl wisps.

In the Cenomanian and Turonian Chalks of the Paris Basin Deconinck & Chamley (1995) have taken a different approach. They studied the smectitic phases in chalks and marls where there is either local or general geological evidence of the origin of the clay assemblages. They examined (a) the smectite-rich clay assemblages in the Early Cenomanian Chalk which have acid-insoluble residues of 30% and more of the total sediment and much of this is smectite; these chalks lack any obvious evidence of a volcanic origin; (b) smectite-rich clay assemblages in the Late Cenomanian chalks where the total acid insoluble residue makes up only a small proportion of the sediment (~2%); and (c) interbedded thin marls and beds of chalk (15% acid insoluble residues) of Turonian age where there is clear evidence (presence of feldspar phenocrysts and Eu anomalies in their *REE* patterns) that the clay assemblage of the marl seams originated by the *in situ* argillisation of volcanic ash. Two main types of are recognized, a Mg-rich dioctahedral illite-smectite with 80−100% smectite layers displaying a second endothermic reaction in the region between 600−700ºC and a K_2O-rich dioctahedral illite-smectite with 65−95% smectite layers with its second endothermic reaction between 500 and 550ºC. Both types may occur as fleecy crystals whereas the K_2O-rich variety occurs also as lath-shaped crystals with an enhanced K_2O content − no doubt this represents the recrystallization of an originally fleecy morphology.

Comparison of the results from the Paris Basin with those from Denmark suggests that the *high-smectite/illite-smectite mixed-layer* (HS/I-S) and the *low-smectite/illie-smectite mixed-layer* (LS/I-S) described by Lindgreen *et al.* (2002, 2008) and Drits *et al.* (2004) may be equivalent to, respectively, the volcanogenic I-S and the detrital I-S phases described by Deconinck & Chamley (1995). The chlorite-containing mixed-layer phases recorded from the Danish chalk either do not occur or have not been identified in the Cenomanian and Turonian Chalk of the Paris Basin.

Our approach to investigate the origin and variation in the smectitic phases present in the Chalk has been more circumspect. The first part of our investigation reported in this paper has dealt with the relationship between the overall mineralogy of the different particle size fractions within the clay assemblages and how this is related to the

extent and type of calcite cementation and its geological setting. Already at this stage of our study considerable progress has been made on two fronts. At Peacehaven, in the high-purity chalk of Campanian age the lack of a early Mg-rich calcite cement may be related to the development of trioctahedral and dioctahedral smectitic phases irrespective of whether it is considered to be volcanogenic or detrital in origin. In the Cenomanian Chalk at Hunstanton and Speeton there is evidence of some correlation between the type and timing of calcite cementation and the heat stability of the dioctahedral smectitic phase on heating at 400ºC. The next stage of our investigation will be the examination of the chemistry, thermal characteristics, and morphology of the smectitic phases separated in this study.

REFERENCES

Brigatti M.F. (1983) Relationships between composition and structure in Fe-rich smectites. *Clay Minerals*, **18**, 177−186.

Brindley G.W. & Wan H.-M. (1974) Use of long spacing alcohols and alkanes for calibration of long spacings from layer silicates, particularly clay minerals. *Clays and Clay Minerals*, **22**, 313−317.

Deconinck J.F. & Chamley H. (1995) Diversity of smectite origins in Late Cretaceous sediments: Examples of chalks from Northern France. *Clay Minerals*, **30**, 365−379.

Drits V.A. & McCarty D. (1996) A simple technique for a semi-quantitative determination of the trans-vacant and cis-vacant in 2:1 layer contents in illites and illite-smectites. *American Mineralogist*, **81**, 852−863.

Drits V.A., Lindgreen H., Salyn A.L., Ylagan R. & McCarty D.K. (1998) Semiquantitative determination of trans-vacant and cis-vacant 2:1 layers in illites and illite-smectite by thermal analysis and X-ray diffraction. *American Mineralogist*, **83**, 1188−1198.

Drits V.A., Lindgreen H., Sakharov B.A., Jakobsen F. & Zviagina B.B. (2004) The detailed structure and origin of clay minerals at the Cretaceous/Tertiary boundary, Stevns Klint (Denmark). *Clay Minerals*, **39**, 367−390.

Gallois R.W. (1994) Geology of the country around King's Lynn and the Wash. *Memoir of the British Geological Survey.* Sheet 145 and part of 129 *(England and Wales)*, 210pp.

Greene-Kelly R. (1957) The montmorillonite minerals (smectite). Pp. 140−164 in: *The Differential Thermal Analysis of Clays* (R.C. Mackenzie, editor). Monograph of the Mineralogical Society, London.

Hu X.F., Jeans C.V. & Dickson J.A.D. (2012) Geochemical and stable isotope patterns of calcite cementation in the Upper Cretaceous Chalk, UK: Direct evidence from calcite-filled vugs in brachiopods. *Acta Geologica Polonica*, **62**, 143−172.

Hu X.F., Long D. & Jeans C.V. (2014) A novel approach to the study of the development of the Chalk's smectite assemblage. *Clay Minerals*, **49**, 277−297.

Jeans C.V. (1968) The origin of the montmorillonite of the European Chalk with special reference to the Lower Chalk of England. *Clay Minerals*, **7**, 311−329.

Jeans C.V. (1980) Early submarine lithification in the Red Chalk and Lower Chalk of eastern England: a bacterial control model and its implications. *Proceedings of the Yorkshire Geological Society*, **43**, 81−157.

Jeans C.V. (2006) Clay mineralogy of the British Cretaceous. *Clay Minerals*, **41**, 47−150.

Jeans C.V., Hu X.F. & Mortimore R.N. (2012) Calcite cements and the stratigraphical significance of the marine $\delta^{13}C$ carbonate reference curve for the Upper Cretaceous Chalk of England. *Acta Geologica Polonica*, **62**, 173−196.

Kawano M. & Tomita K. (1991) Dehydration and rehydration of saponite and vermiculite. *Clays and Clay Minerals*, **39**, 174−183.

Lindgreen H., Drits V.A., Sakharov B.A., Jakobsen H.J., Salyn A.L., Dainyat L.G. & Krøyer H. (2002) The structure and diagenetic transformation of illite-smectite and chlorite-smectite from North Sea Cretaceous-Tertiary chalk. *Clay Minerals*, **37**, 429−450.

Lindgreen H., Drits V.A., Jakobsen F. & Sakharov B.A. (2008) Clay mineralogy of the central North Sea Upper Cretaceous-Tertiary chalk and the formation of clay-rich layers. *Clays and Clay Minerals*, **56**, 693−710.

Mackenzie R.C. (1970) Simple phyllosilicates based on gibbsite- and brucite-like sheets. Pp. 497−537 in:

Differential Thermal Analysis (R.C. Mackenzie, editor), **1**. Academic Press, London.

Mackenzie R.C. (1972) *Differential Thermal Analysis*, **2**. Academic Press, London.

Moore D.M. & Reynolds R.C. Jr. (1997) *X-ray Diffraction and the Identification and Analysis of Clay Minerals*. New York: Oxford University Press.

Perrin R.M.S. (1964) The analysis of Chalk and other limestones for geochemical studies. Pp. 208−221 in: *Analysis of Calcareous Materials*. Monograph of the Society of Chemical Industry (London), **18**, 481 pp.

Reynolds R.C. Jr. & Reynolds R.C. III (1996) *NEWMOD for Windows.* The calculation of one dimensional X-ray diffraction patterns of mixed-layered clay minerals: Hanover, NH.

Wolters F. & Emmerich K. (2007) Thermal reactions of smectites − relation of dehydroxylation temperature to octahedral structure. *Thermochimica Acta*, **462**, 80−88.

Wolters F., Lagaly G., Kahr G., Kueesch R. & Emmerich K. (2009) A comprehensive chacterization of dioctahedral smectites. *Clays and Clay Minerals*, **57**, 115−133.

Wright, C.W. (1935) The Chalk rock fauna in East Yorkshire. *Geological Magazine*, **72**, 441−442.

Young B.R. (1965) X-ray examination of insoluble residues from the Chalk. Appendix D in: The Leatherhead (Fetcham) Borehole (D.A. Gray). *Bulletin of the Geological Survey of Great* Britain, **23**, 110−114.